

Guidelines for Avoiding Vortex Wakes During Use of Closely Spaced Parallel Runways

*Vernon J. Rossow and Larry A. Meyn
Ames Research Center
Moffett Field, California*

The NASA STI Program Office . . . in Profile

Since its founding, NASA has been dedicated to the advancement of aeronautics and space science. The NASA Scientific and Technical Information (STI) Program Office plays a key part in helping NASA maintain this important role.

The NASA STI Program Office is operated by Langley Research Center, the Lead Center for NASA's scientific and technical information. The NASA STI Program Office provides access to the NASA STI Database, the largest collection of aeronautical and space science STI in the world. The Program Office is also NASA's institutional mechanism for disseminating the results of its research and development activities. These results are published by NASA in the NASA STI Report Series, which includes the following report types:

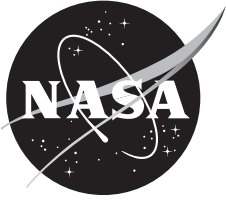
- **TECHNICAL PUBLICATION.** Reports of completed research or a major significant phase of research that present the results of NASA programs and include extensive data or theoretical analysis. Includes compilations of significant scientific and technical data and information deemed to be of continuing reference value. NASA's counterpart of peer-reviewed formal professional papers but has less stringent limitations on manuscript length and extent of graphic presentations.
- **TECHNICAL MEMORANDUM.** Scientific and technical findings that are preliminary or of specialized interest, e.g., quick release reports, working papers, and bibliographies that contain minimal annotation. Does not contain extensive analysis.
- **CONTRACTOR REPORT.** Scientific and technical findings by NASA-sponsored contractors and grantees.

- **CONFERENCE PUBLICATION.** Collected papers from scientific and technical conferences, symposia, seminars, or other meetings sponsored or cosponsored by NASA.
- **SPECIAL PUBLICATION.** Scientific, technical, or historical information from NASA programs, projects, and missions, often concerned with subjects having substantial public interest.
- **TECHNICAL TRANSLATION.** English-language translations of foreign scientific and technical material pertinent to NASA's mission.

Specialized services that complement the STI Program Office's diverse offerings include creating custom thesauri, building customized databases, organizing and publishing research results . . . even providing videos.

For more information about the NASA STI Program Office, see the following:

- Access the NASA STI Program Home Page at <http://www.sti.nasa.gov>
- E-mail your question via the Internet to help@sti.nasa.gov
- Fax your question to the NASA Access Help Desk at (301) 621-0134
- Telephone the NASA Access Help Desk at (301) 621-0390
- Write to:
NASA Access Help Desk
NASA Center for AeroSpace Information
7115 Standard Drive
Hanover, MD 21076-1320



Guidelines for Avoiding Vortex Wakes During Use of Closely Spaced Parallel Runways

*Vernon J. Rossow and Larry A. Meyn
Ames Research Center
Moffett Field, California*

National Aeronautics and
Space Administration

Ames Research Center
Moffett Field, California 94035-1000

Available from:

NASA Center for AeroSpace Information
7115 Standard Drive
Hanover, MD 21076-1320
(301) 621-0390

National Technical Information Service
5285 Port Royal Road
Springfield, VA 22161
(703) 487-4650

TABLE OF CONTENTS

LIST OF FIGURES	iv
NOMENCLATURE	v
SUMMARY	1
I. INTRODUCTION	1
A. Background	1
B. Application to Closely Spaced Parallel Runways.....	3
II. MOVEMENT AND SPREAD OF WAKE-HAZARDOUS REGIONS	4
A. Size of Wake-Hazardous Region Around Initial Location of Vortex Pair	5
B. Spread of Wake-Hazardous Region by Turbulence.....	7
C. Wake Spreading by Long-Wave Instability.....	11
D. Self-Induced Downward and Lateral Movement of Vortex Pair.....	14
E. Long-Term Self-Induced Spreading by Turbulence	15
F. Movement of Wake-Hazardous Boundaries by Wind and Gusts	16
G. Effect of Robust Jet-Engine Exhaust Plumes on Wake Dynamics	17
III. COMPUTATIONAL RESULTS.....	18
A. Equations for Wake Spreading	18
B. Computer Program for Estimation of Wake Spreading.....	20
IV. IMPLICATIONS FOR AIRPORT OPERATIONS	22
V. CONCLUSIONS.....	24
VI. REFERENCES	25
APPENDIX: COMPUTER CODE FOR WAKE-SPREADING ESTIMATES	31

LIST OF FIGURES

Figure 1.	Safe and unsafe along-trail separation distances for following aircraft brought about by intrusion of wake shed by leading aircraft.	4
Figure 2.	Contours of constant wake-induced rolling-moment coefficient used to define initial boundaries of hazardous region; $C_{Lg} = 1.5$, $b_f/b_g = 0.29$, and maximum $C_{lfmax} = 0.12$	6
Figure 3.	Plan view of contributions to spread of wake-hazardous region as a function of time/distance behind generating wing; $b_f/b_g \leq 0.5$	8
Figure 4.	Comparison of predicted linking times as a function of magnitude of disturbance velocities from atmospheric turbulence for long-wave instability of a vortex pair in terms of parameters used by Crow and Bate (ref. 43) and by Sarpkaya (ref. 49).	12
Figure 5.	Velocity-based estimate for linking time as a function of magnitude of disturbance velocity for long-wave instability of a vortex pair plotted on linear scales in terms of parameters recommended for applications.	13
Figure 6.	Method used to move cross-sectional boundaries of wake-hazardous region in response to lateral and vertical wind and turbulence disturbance velocity components.	16
Figure 7.	Plan view of components of wake-hazardous region shed by B-747 with numbered markers to indicate where various wake-spreading events take place. Computed by using the computer program listed in the appendix with $\epsilon_{eff} = 0.05$ and $V_{errfs} = 5$ ft/s (1.52 m). All other wind components are assumed to be of negligible magnitude.	21
Figure 8.	Plan view of components of wake-hazardous region shed by B-737 with numbered markers to indicate where various wake-spreading events take place. Computed by using the computer program listed in the appendix with $\epsilon_{eff} = 0.05$ and $V_{errfs} = 5$ ft/s (1.52 m). All other wind components = 0.	22

NOMENCLATURE

a	peak-to-peak amplitude of long-wave instability, ft (m)
A	a/b_g
b	wing span, ft (m)
b'	span wise distance between vortex centers $\approx \pi b_g/4$, ft (m)
B _{hz}	breadth of hazardous part of wake region to be avoided, ft (m)
C _L	lift coefficient = Lift/ $q_\infty S$
C _l	rolling moment coefficient = Rolling moment/ $q_\infty S b$
D _{hz}	depth of hazardous part of wake region to be avoided, ft (m)
GPS	Global Positioning System
Kn	knots
G	$\Gamma/b_g U_\infty$
q _∞	$\rho_\infty U_\infty^2/2$
S	plan form area of wing, ft ² (m ²)
t	time, s
T _g	τG
x	distance in flight or longitudinal direction, ft (m)
y, z	distance in lateral and vertical directions, ft (m)
u, v, w	velocity components in x, y, and z directions, ft/s (m/s)
U _∞	velocity of wake-generating aircraft, ft/s (m/s)
Wt	weight, lbs (N)
Δt	time interval between wake-generating and following aircraft
ε	turbulence level or eddy-dissipation rate
Γ	centerline circulation on wing, ft ² /s (m ² /s)
θ	angle between vertical and plane of waves, degrees
ρ	air density, slugs/ft ³ (kg/m ³)
τ	time parameter = tU_∞/b_g

NOMENCLATURE (cont.)

Subscripts

o	initial value
decomp	decomposing wake
eff	effective
f	following aircraft
fil	vortex filament
g	wake-generating or leading aircraft
grdef	ground effect
Lnk	linking of vortex pair
lw	long-wave instability of vortex pair
max	maximum
min	minimum
ops	operations
oval	streamline oval that encloses vortex pair
pln	plan view
pr	vortex pair
rnwy	runway
spred	wake-spreading amount
t	turbulence
wnd	wind
∞	free-stream condition

GUIDELINES FOR AVOIDING VORTEX WAKES DURING USE OF CLOSELY SPACED PARALLEL RUNWAYS¹

Vernon J. Rossow² and Larry A. Meyn³

Ames Research Center

SUMMARY

A method is proposed for the estimation of the movement and spread of lift-generated vortex wakes as a function of time to better enable aircraft arriving at airports to avoid the hazards associated with the wakes of preceding aircraft. Operations on closely spaced parallel runways are used to illustrate how the method may be applied. The paper begins with an overview of the aerodynamic mechanisms that cause the hazardous parts of lift-generated wakes to spread and to move as a function of time. A computational method is then presented for the determination of the spread and movement of the hazardous parts of vortex wakes as a function of time during operations of aircraft as they approach closely spaced parallel runways for a landing. The results suggest guidelines for efficiently and effectively avoiding the vortex wakes of preceding aircraft. Because uncertainties occur in the theoretical tools developed and in the measurements made of the components of the time-averaged wind and its gust magnitudes, flight tests are recommended to confirm and refine the guidelines presented, and to verify the techniques used to measure the atmospheric parameters that control intrusion of the hazardous elements of lift-generated wakes into nearby parallel runways.

I. INTRODUCTION

A. Background

If the lift-generated wakes of aircraft were not hazardous, and did not persist for several minutes behind the generating aircraft, runways could be safely located close to each other and re-used within time intervals based only on air-traffic management constraints rather than on aerodynamic ones that relate to flight safety (ref. 1). Because lift-generated wakes do pose a hazard, studies have been conducted on ways to reduce the effect of vortex wakes on airport capacity (refs. 1–50). One such method considers the transport and decay of vortex wakes as a function of time as a means to shorten the time required for single runways to become vortex free, and therefore, safe for reuse (refs. 2–11). It was found that the capacity of a single runway might then be increased by as much as 10% by judicious use of weather information and aircraft timing. Although beneficial, such an improvement does not accommodate the factor of two or

¹ Presented as AIAA-2008-6907 at 26th AIAA Applied Aerodynamics Conference, Honolulu, HI, Aug. 18-21, 2008.

² Ames Associate, Aviation Systems Division, Ames Research Center, Moffett Field, CA 94035-1000.

³ Ames Research Center, Moffett Field, CA 94035-1000.

three increase in traffic volume that is expected during the next 20 years. It was therefore reasoned that improvements in the use of a single runway would not achieve the desired goal and that the number of runways at each airport will need to be increased to accommodate the predicted need.

An increase in the number of runways at most airports is usually not possible if the runways are built with the conventional lateral spacing of 4300 ft (1311 m) so that they can be operated independently. Because available land area at or near existing airports is already in short supply, recent research has focused on the use of closely spaced parallel runways, which are often spaced parallel to each other at distances as small as 750 ft (230 m). The runways are then too close to operate independently, because wakes shed by preceding aircraft on one runway might intrude into the air space to be used by a following aircraft on a nearby runway. Management of aircraft flight paths will then require more planning because of the proximity of aircraft to one another during landing operations, and because of the higher density of aircraft traffic on the ground and in the air at and near airports. Although sometimes advantageous, stagger built into closely spaced runways is not considered in this paper.

The research reported addresses the development of a method for estimation of the rate at which lift-generated vortex wakes of subsonic transport aircraft move and spread because of wind currents, turbulence in the atmosphere along the flight path of arriving aircraft, and self-induced spreading mechanisms. Previous studies have examined the details of various aerodynamic mechanisms that cause the vortex wakes of subsonic aircraft to spread and move (refs. 12–50). Guidelines developed by use of the knowledge presented in the foregoing studies make it possible to reliably predict how lift-generated vortex wakes move and spread as a function of time. A preliminary description of that work was described in a previous paper that was presented at a technical meeting (ref. 51). The purpose of the paper, and its presentation at the technical meeting, was to use the research conducted on wake-spreading and -movement mechanisms for lift-generated vortex wakes to provide a reliable estimate for the time at which the vortex wake of a leading aircraft will intrude into the airspace of a following aircraft that is scheduled to land on a nearby, closely spaced parallel runway.

The foregoing paper (ref. 51) on the movement and spread of vortex wakes assumed that the jet engines on the wake-generating aircraft were at idle for the approach and landing being analyzed. After publication of that paper, a study was made of the effect of robust engine thrust on wake spreading as a function of time (refs. 52 and 53). Observations of condensation trails behind aircraft flying at cruise altitudes showed that robust thrust brings about a linking mechanism in the vortex pair shed by aircraft that differs from the one assumed by Crow (refs. 42 and 43). That is, the presence of robust engine thrust (as occurs with engines on aircraft flying at cruise altitudes) first initiates a sequence of circumferential vortex rings around the energetic exhaust plumes. When the trailing vortex pair has descended to the bottom of the combined exhaust plumes that are just above the inside bottom of the sequence of vortex rings that surround the merged exhaust plumes of the engines, the in and out velocity field of the vortices induces a train of vertical waves on the trailing vortex pair. The train of waves induced on the vortex filaments then re-forms to bring about across-span linking events that form a chain of vortex loops that is easily recognized as the same as the vortex loops associated with the long-wave instability (ref. 42). However, the time required for linking process that brings about the

destruction of the hazardous structure of a vortex pair is now longer by as much as a minute or more than the atmospheric turbulence process (refs. 52 and 53). The reason for the added time comes about because the vortex pair must first descend from near the center of the wake to the bottom of the merged exhaust plumes and then re-form the wave train structure for the linking process.

Therefore, robust engine thrust changes two characteristics in the spreading rate of lift-generated vortex wakes. First, because robust engine thrust delays rather than advances the initiation of the long-wave instability, the analysis presented in the meeting paper (ref. 51) is still the appropriate process for use in the time-dependent computation of wake spreading. It must be remembered, however, that when engine thrust is robust, the longer time interval observed for initiation of the long-wave instability causes the wake hazardous region to spread more slowly and to endure for a longer period of time than when initiated by ambient turbulence. As a consequence, the recycle time for a given set of runways will be increased when robust engine thrust is used by any aircraft in the group while on approach to a runway for a landing.

B. Application to Closely Spaced Parallel Runways

The remainder of this paper focuses on estimation of the spreading of vortex wakes by all of the mechanisms identified so far and on the impact that the spreading has on the allowable spacing between two aircraft making nearly simultaneous approaches. This paper does not address the recycle time of the runway system. Therefore, this section discusses the time interval between aircraft passage and the intrusion of vortex wakes shed by a leading aircraft into the airspace of a following aircraft.

The use of closely spaced parallel runways is not new. At present, operations are conducted as nearly simultaneous landings during visual meteorological conditions (VMC). Encounters with vortex wakes are then safely avoided because the along-trail spacing (or time) between aircraft landing on two closely spaced parallel runways is too small for the vortex wake shed by either aircraft to spread enough to intrude into the airspace of the other aircraft until after both have landed (fig. 1). Therefore, an aerodynamic wake-avoidance problem has been solved by use of simultaneous operations of arriving aircraft. The purpose of the research presented here is to call attention to the fact that aircraft pairs need not be simultaneous, but may also land safely with in-trail spacings of 10 s or more when atmospheric conditions provide circumstances that produce slow rates of wake spreading.

Because nearly simultaneous landing of aircraft pairs now depends on the ability of both aircraft to see each other, visibility degradation requires that runway operations be changed to instrument conditions (IMC). When this situation occurs, only one of the two closely spaced parallel runways is used. The landing capacity of the runway pair is then reduced to half of its clear-weather value so that the capacity of the two runways is the same as that of single-runway operation. Efforts have been under way for some time to enable two aircraft to safely conduct nearly simultaneous landings during IMC so that operations can be carried out under all visibility conditions. One issue is that an in-trail separation buffer is required during IMC for safe

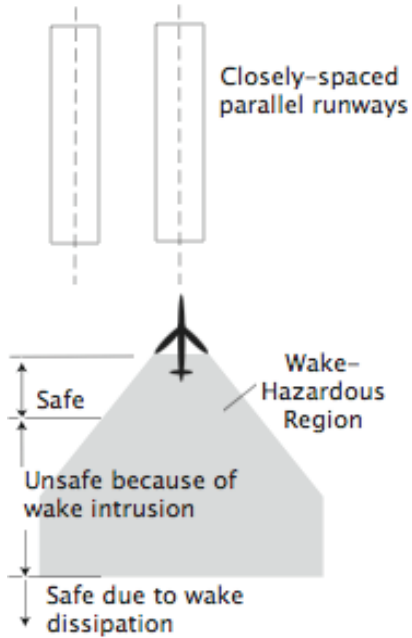


Figure 1. Safe and unsafe along-trail separation distances for following aircraft brought about by intrusion of wake shed by leading aircraft.

operations. Research with piloted simulators has shown that along-trail time intervals between aircraft in a pair during IMC can be safely decreased to five s (refs. 31 and 54–63) when pilots are able to rely totally on electronic guidance that assures safe separation between aircraft in a group that is landing on closely spaced runways.

The aerodynamic mechanisms that bring about wake spreading as a function of time, and the way that atmospheric conditions affect this aerodynamic problem (refs. 12–20), are summarized in the next section to develop a reliable computational method for prediction of the duration of the safe zone illustrated in figure 1. The results presented assume that the transition from a VMC to an IMC capability at airports has been completed (refs. 21–33). For numerous operational reasons, success with wake-avoidance technologies is achieved when the safe zone for the along-trail separation distance, or time between the two aircraft, can be safely increased from nearly simultaneous (or 5 s, i.e., about 1000 ft or 305 m) to as much as 10 s (about 2000 ft or 610 m) or more. Larger along-trail separation distances facilitate wave-off operations and accommodate the grouping of aircraft pairs. Estimates made by use of a computer program presented in the appendix indicate that the safe zone associated with side-by-side approaches can usually be safely increased to 10 s or more if the smaller aircraft in the pair is the leading aircraft and if the following aircraft lands upwind of the leading aircraft when a side wind is present.

II. MOVEMENT AND SPREAD OF WAKE-HAZARDOUS REGIONS

The wake-intrusion time depicted in figure 1 depends on the lateral separation distance between the runways, the sizes of the aircraft involved, the time-averaged wind magnitude and direction, and the turbulence magnitude in the atmosphere where the wake of the generating aircraft is

deposited. It is noted that only the lateral extent and location of wake-hazardous regions are studied because the altitudes of the two aircraft on approach to a set of parallel runways are usually close to the same at a given station along their approach paths, thereby reducing the problem to a lateral one. Only an overview of previous results is presented here because considerable attention has already been given to the details of the aerodynamics of how vortices move and spread (refs. 12–20, 52, and 53). The analysis here divides the movement and spread of lift-generated vortex wakes by aerodynamic means into the following mechanisms:

- A. Size of wake-hazardous region around initial location of vortex pair
- B. Spread of wake-hazardous region by turbulence
- C. Wake spreading by long-wave instability initiated by atmospheric turbulence
- D. Self-induced downward and lateral movement of vortex pair
- E. Long-term self-induced spreading by turbulence
- F. Movement of wake-hazardous boundaries by wind and gusts
- G. Effect of robust jet-exhaust plumes on wake dynamics

Any deviations by the wake-generating aircraft in a vertical or horizontal direction from the intended flight path are assumed to be small enough that they have a negligible effect on wake spreading, and are therefore not included in the computations. It is noted that any wake spreading brought about by the effect of engine thrust on wake dynamics was not included in the foregoing list as published in the meeting version of the paper (ref. 51). Section II-G to follow describes research carried out after publication of the meeting version of the paper (refs. 52 and 53). Because it was found that the initiation of the long-wave instability by robust engine thrust requires more time than when initiated by ambient turbulence, the formulation presented in the meeting paper remains the more conservative process and should continue to be used to estimate the spreading and decomposition of lift-generated vortex wakes of aircraft during approach to airport runways.

A. Size of Wake-Hazardous Region Around Initial Location of Vortex Pair

The center of either of the two vortices in the pair shed by a preceding aircraft is the most hazardous location for an encounter. As indicated in figure 2, the hazard extends with decreasing intensity for some distance away from the center of each of the two vortices in the pair. The figure presents a cross-sectional view of the lines of equal rolling-moment coefficient, C_{lf} , that have been induced on a following wing of rectangular plan form as a function of spanwise and vertical distances made dimensionless by use of the span of the wake-generating wing, b_g . The lift coefficient on the wake-generating wing is represented by the symbol C_{Lg} , and the span of the following wing is given by b_f . One of the more important parameters that governs the magnitude of the wake-induced rolling moments is the ratio of the span of the following wing to that of the wake-generating wing, b_f/b_g . A wake-hazardous region is therefore defined as that part of the atmosphere that must be avoided by following aircraft because hazardous elements of a lift-generated vortex pair shed by a preceding aircraft, and the hazard they pose, are located

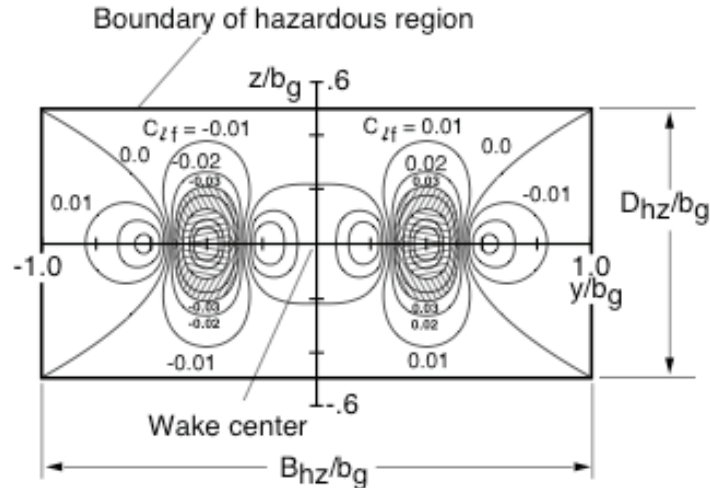


Figure 2. Contours of constant wake-induced rolling-moment coefficient used to define initial boundaries of hazardous region; $C_{L_0} = 1.5$, $b_f/b_g = 0.29$, and maximum $C_{l_{fmax}} = 0.12$.

therein to within a high degree of certainty (refs. 34–37). The term wake-hazardous region is used to describe the region to be avoided because, if the centerline of a following aircraft is outside the boundary of a given hazardous region, any disturbances induced on a following aircraft by the vortex wake of a preceding aircraft are indistinguishable from an encounter with ambient atmospheric turbulence in the area, which is easily controllable with the ailerons on the encountering aircraft.

Because the vortex-induced rolling moment fades approximately as the square of the distance from the center of the wake, the choice of a maximum tolerable vortex-induced rolling moment is somewhat arbitrary (refs. 1 and 34–37). The present study uses the specification that the centerline of the following aircraft must be far enough from the centerline of the wake generated by a preceding aircraft so that it does not encounter a vortex-induced rolling moment larger than one-sixth of the roll-control authority available by use of the ailerons. This definition is based on simulated encounters with vortex wakes that indicate that the following aircraft will not roll more than 5° if the vortex-induced rolling moment is less than one-half of the roll-control authority on the aircraft (ref. 34). The one-sixth value is used instead of the one-half value because it is more conservative and does not greatly increase the size of the region to be avoided.

The contours of equal vortex-induced rolling moment shown in figure 2 were calculated theoretically and confirmed by wind-tunnel experiments (refs. 34–37). The calculations carried out to generate figure 2 assume that the flow field in which the vortices are embedded is steady with time (i.e., no wind or turbulence). The contours shown are based on a combination of theory and experimental confirmation at a time, or short distance, behind the wake-generating aircraft where the wake can be considered as rolled up. When the vortex sheet shed by the wing has rolled up, the vortex wake, and the hazard that it poses, is noted to extend out beyond the wing tips of the wake-generating aircraft. Lines of constant vortex-induced rolling-moment coefficient then have a well-defined structure that changes slowly with time. The centers of the vortex pair that drive the over-turning velocity distribution in the wake remain in about the same relative location until three-dimensional disturbances begin the process of wake decomposition. Before

that time, the contours of constant rolling-moment coefficient shown in figure 2 approximate the steady-state, or time-averaged, values that would be experienced by aircraft in an actual flight situation.

At aircraft span ratios larger than $b_f/b_g = 0.29$, the dimensionless size of a box that encloses the 0.01 rolling-moment contours is roughly constant until the span ratio exceeds 0.5. For example, when the span ratio is equal to 1.0, computed contours of equal rolling moment, like those shown in figure 2, indicate that the size of the hazardous region is about $2.5 b_g$ in breadth and one span or b_g in depth (refs. 13 and 34). To have a continuous relationship for the initial size of the hazardous region as a function of span ratio, the span wise breadth is approximated by $B_{hz0} \approx 2 b_g$ when $b_f/b_g < 0.5$, where B_{hz0} is the breadth of the hazardous region a short distance behind the wake-generating aircraft. When $b_f/b_g \geq 0.5$, the breadth of the hazardous region is approximated by

$$B_{hz0} \approx [2 + (b_f/b_g - 0.5)] b_g \quad (1)$$

The initial depth of the hazardous region, $D_{hz}(t)$, is roughly constant at one span, independent of span ratio. The initial hazardous region is, of course, centered on the centerline of the wake-generating aircraft at the time that it was generated, but rapidly becomes offset laterally because of the steady-state component of the ambient wind, and vertically because of the self-induced downward motion of the wake, estimated as

$$w_{pr} = -|\Gamma_{ac}|/2\pi b' \quad (2)$$

where w_{pr} is the initial value of the self-induced downward velocity of the vortex pair; Γ_{ac} is the centerline circulation bound in the wing of the wake-generating aircraft, which is equal to the circulation content of each of the two vortices in the pair; and b' is the span wise distance between the centroid of circulation for each of the two vortices in the pair (usually about $\pi b_g/4$).

B. Spread of Wake-Hazardous Region by Turbulence

When vortex wakes are embedded in a quiescent fluid, like a water tow tank, the vortices remain relatively straight and decompose slowly. The two vortices then begin their trails as straight lines from near the wingtip regions at about $y/b_g = \pm\pi/8$, as indicated by the straight lines labeled as “Undisturbed vortices” in figure 3. The quantity y/b_g is the dimensionless spanwise distance from the center of the wake-hazardous region. As described in the previous section, the initial breadth of the wake-hazardous region is $B_{hz}(0) = 2b_g$, when, $b_f/b_g \leq 0.5$. The sides of the hazardous region are labeled as “Initial sides of hazardous region” in figure 3. The other lines in the figure indicate the outboard boundaries of the hazardous region due to contributions directly or indirectly related to the turbulence in the air where the vortices are embedded. A turbulent flow field is defined as one wherein the flow field has random unsteady motions superimposed on its time-averaged orderly motion (ref. 38). The unsteady-random motions are eddies or swirling motions whose sizes vary from smaller than the wing chord up to numerous span lengths. The magnitude of these velocity perturbations relative to the flight velocity of the aircraft is usually small.

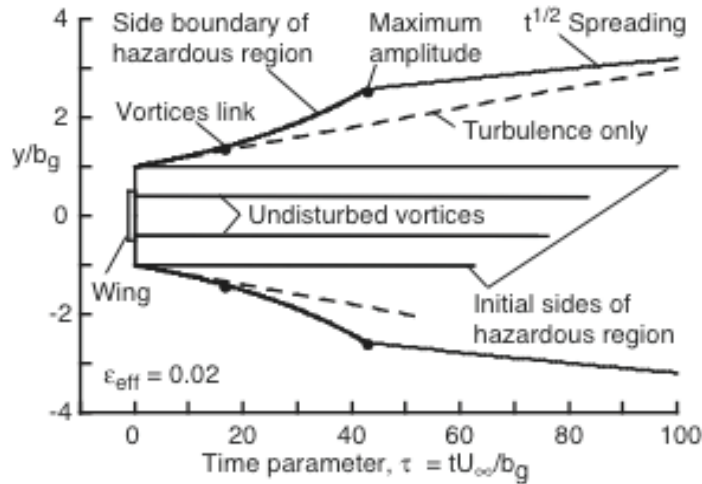


Figure 3. Plan view of contributions to spread of wake-hazardous region as a function of time/distance behind generating wing; $b_f/b_g \leq 0.5$.

Three sources of turbulence are usually present in the region occupied by the vortices after being shed by the lifting surfaces on a wake-generating aircraft. The first source is from the atmosphere through which the aircraft is flying. The turbulence from the second source is placed in the wakes of aircraft by the aircraft itself, which includes its various lifting surfaces. The sizes of the eddies generated on the surfaces of the airframe go from very small in the viscous boundary layer on the surface of the aircraft to a fraction of a wingspan in regions of flow separation or engine exhaust. Trailing vortices are coherent and organized in structure and so are not considered sources of turbulence until the highly organized structure of vortex wakes begins to decompose and decay.

The third source of turbulence consists of flow disturbances generated by the energized streams from the propulsion system on board the wake-generating aircraft. Jet-induced disturbances usually go directly into the region occupied by the rolled-up vortices and can therefore become an important source for disturbances that are able to modify the structure of vortices shed by the wing (see section II-G). Immediately behind the aircraft, the jet structures consist of highly energized cores with sharply defined cylindrical shear layers surrounding them. About one span behind the aircraft, the sides of the jet streams begin to break up into turbulent eddies that grow from quite small at jet exits into eddies that are about the size of the wingspan of the aircraft—or larger. As the dominant eddies grow in size, their swirl velocities become smaller until the turbulence within the wake becomes dispersed over a large region that grows roughly as the square root of time (ref. 39). Eventually, the velocity magnitudes in the wake become difficult to distinguish from those in nearby atmospheric turbulence. During the change in jet-exhaust streams from an orderly high-speed stream to eventual dispersion, each exhaust stream is surrounded by an array of circumferential vortices that act like rollers between the jet streams and the nearly stationary atmosphere. As part of the dissipation process, the individual jet streams merge to form a single turbulent stream with a single array of irregularly shaped circumferential vortices that are sometimes visible in condensation trails of aircraft flying at cruise altitudes (ref. 53).

The time-averaged magnitude of the various unsteady random motions in which the vortex wake is embedded is called the turbulence level of the fluid. The intensity of the turbulence is usually found by measuring the magnitudes of the root-mean-squared value of the time-dependent velocity perturbations. The turbulence level of the flow field is then the ratio of such a measurement divided by a characteristic velocity of the steady motions. For example, in wind tunnels the time-averaged turbulence level, ϵ_t , is determined by measuring the time-averaged disturbance velocities (barred and primed quantities) along the three axes over a large unit of time, like a minute or more, and then dividing the result by the square of the free-stream velocity (ref. 38).

$$\epsilon_t = [(\overline{u'}^2 + \overline{v'}^2 + \overline{w'}^2)/3U_\infty^2]^{1/2} \quad (3)$$

The three primed and barred quantities inside the set of parentheses represent the time-averaged values of the square of the three components of the measured perturbation velocities in the air stream of the empty wind tunnel. The quantity U_∞ is the time-averaged velocity of the air stream, which is in the x-direction and aligned with the centerline of the wind tunnel (refs. 40 and 41). The subscript t is used to denote that the parameter ϵ is associated with the turbulence in the airstream and not some other unsteady feature of the flow field.

Of interest here is the fact that the turbulence in the air stream, no matter what the source, causes segments of vortex wakes to migrate randomly so as to spread wake segments, and their hazardous character, to locations outside of the initial boundaries of the wake-hazardous region. The time-averaged outer boundary of the spread of vortex centers with downstream distance is shown in plan view in figure 3 by the two dashed lines for a turbulence level of $\epsilon_t = 0.02$. The beginning points of the two dashed lines are noted to be at the maximum lateral location of the initial size of the wake-hazardous region, rather than at the span wise location where the vortices originate. This relocation is done because any span wise or lateral change in vortex location causes the outer boundary of the hazardous region to change as well. Because only the outer boundary of the wake-hazardous region is of interest, any increase in the lateral location of a vortex center must be added onto the maximum breadth of the hazardous region. It is thereby assumed that the structure of a vortex is largely unchanged by its movement. These two assumptions may be overly conservative, but are recommended to be certain of the reliability of the level of safety represented by the outermost boundaries of the wake and its movement.

Other than an intuitive realization that turbulence causes trailing vortices to become sinuous with time, and therefore causes vortex elements to spread as a function of time, the only quantitative experimental evidence that vortices meander about because of turbulence in the ambient flow field is found in some wind tunnel experiments (refs. 35 and 36). The wind tunnel experiments were used to obtain measurements of the structure of lift-generated vortex wakes of transport aircraft at various downstream distances behind the aircraft model. It was found that turbulence in the region where the vortices were embedded did slowly change the structure of the vortices, but the largest influence was that turbulence in the ambient stream caused an across-stream unsteady and random motion (or meander) of the vortex centers in the 40- by 80-Foot and 80- by 120-Foot Subsonic Wind Tunnels at NASA Ames Research Center. The magnitude of the meander distance was found to increase linearly with downstream distance, and thereby spread

the hazardous region of the wake at a linear rate. The linear outboard movement of the sides of the hazardous region is therefore justified.

Because atmospheric turbulence structures cannot usually be accurately represented by wind tunnel types of turbulence models, the comparisons being made are recognized as approximate, but more applicable information is not available (ref. 19). Even though accurate comparisons cannot be justified, a qualitative and perhaps quantitative comparison is attempted between the magnitude of wind tunnel turbulence measurements and observed meander distances in the same airstream. Therefore, based on wind tunnel measurements, a value for a vortex-meander-based turbulence level can be evaluated as: $\epsilon_{\text{meand}} = |\bar{v}'|/U_\infty \approx |\bar{w}'|/U_\infty \approx 2/(12 \times 81) \approx 0.002$. Because both wind tunnel facilities have a measured turbulence level of about $\epsilon_t = 0.005$, (refs. 1, 19, 40, and 41), it is found that the maximum values of measured across-stream displacements of the vortex centers are only about 40% of the amount predicted by use of the across-stream time-averaged velocities in the turbulent flow field of the wind tunnel. Although ϵ_{meand} is of the same order of magnitude as the $\epsilon_t = 0.005$ level measured for the turbulence in the free stream and maximum values of meander distance are substantially less, it is not clear how the difference between the two should be reconciled. It is suggested that the difference of the two quantities is brought about by the fact that the swirling velocity for a given eddy in the turbulent flow field does not remain constant but decreases rapidly with time. If true, the average velocity associated with a particular swirling element in the turbulent flow field could be considerably less than the time-averaged perturbation velocities. Whatever the reason for their difference, it is believed that an adjustment constant (i.e., $\epsilon_{\text{meand}}/\epsilon_t = 0.4$) for a relationship between the turbulence measured in the two large wind tunnels and the turbulence that causes meander should not be used at this time because the measured differences are not understood, and because an assumption that maximum meander distances are given by

$$\epsilon_t \approx |v'|_{\text{max}}/U_\infty \approx |w'|_{\text{max}}/U_\infty \quad (4)$$

is more conservative. For this reason, both vortex-meander distance and initiation of the long-wave instability are based on equation (4). Therefore, for wake-spreading computations, it is assumed that $|v'|_{\text{max}}$ and $|w'|_{\text{max}}$ are the representative quantities for reliable (and conservative) prediction of the rate of spread of the hazardous region of vortex wakes as a function of time. Because the most rapid aerodynamic spreading mechanism is the long-wave instability of a vortex pair, the measurements should be taken at all wavelengths between about $2 b_g$ and $10 b_g$ by each wake-generating aircraft as it moves along its approach path to a landing (refs. 42–44). In this way, the worst-case situation is used for both the size of the disturbance and the most effective wavelengths for initiation of the long-wave instability of a vortex pair.

Equation (4) is believed to be more conservative and reliable than some methods used previously to determine typical values for the disturbance velocities for motion of vortex structures (refs. 42, 43, and 49). The earlier methods are based on the fact that the velocity disturbances in various turbulent flow fields tend to have common values for velocity and size that can be modeled by one of several turbulence spectrums. The spectrums relate the velocity field of the turbulence to the wavelength of the disturbance. Although the Kolmogorov turbulence spectrum has often been used to characterize turbulence velocity variations as a function of the wavelength of the

disturbance for numerous time-dependent structures of vortex wakes, its use in the determination of the maximum values for the magnitude of disturbance velocities is believed to be less applicable and reliable than direct measurement of them along the flight path of the wake-generating aircraft. Here and in sections to follow, it will be assumed that the magnitudes of disturbance velocities are found by measurement of the *maximum* values of disturbance velocities taken along the flight path of the wake-generating aircraft over the frequency range where the long-wave instability of Crow is readily initiated.

An equation for the broadening of the wake-hazardous region due to ambient turbulence, without the long-wave instability, is then written as

$$\Delta B_{hzt} = 2\epsilon_{\max} U_{\infty} \Delta t \quad (5)$$

where ΔB_{hzt} is the broadening of the initial wake-hazardous region as caused by turbulence, including vortex meander distances so that ϵ_{\max} is based on the *largest* value found for all of the across-wake perturbation velocities that bring about vortex meander. When vortex spreading is added to the initial breadth of the wake-hazardous region, the boundaries expand as a function of time or distance by the amounts shown by the two dashed lines labeled as “Turbulence only” in figure 3.

C. Wake Spreading by Long-Wave Instability

The long-wave instability of a vortex pair (or Crow instability) comes about when lateral and vertical local sinusoidally shaped displacements are induced on the filaments by turbulence in the region of the atmosphere where the vortices are embedded. The instability has been studied extensively because it decomposes and spreads lift-generated vortex wakes more rapidly than any other known mechanism (refs. 16, 20, and 42–49). If the vortex filaments are not disturbed from a straight-line configuration, the instability does not occur and the vortices trail from the wing as nearly straight lines (fig. 3) when engine power is at low power for approach to a landing. If engine power is at a robust level as for glide-slope adjustments during approach, takeoff, climb, and cruise, it has been found that robust engine power levels cause the long-wave instability to come about by a different mechanism that takes a longer time to develop than when initiated by ambient turbulence (refs. 52 and 53). However, because turbulence along the flight path of aircraft is usually present from one source or another, the vortices first become sinuous and the instability occurs because of ambient turbulence. The growth rate of the instability then depends on the magnitude of the disturbance velocities in a direction across the vortex filaments, which is usually expressed as the intensity of the turbulence where the vortex is embedded (fig. 4). If the turbulence level is low, it takes a long time for the vortices in the pair to link, and if the turbulence is intense, the growth rate of the instability is rapid.

The predictions of vortex linking times when initiated by ambient turbulence as predicted by three theories are presented in figure 4 along with data taken in flight tests (refs. 43 and 44). The data and the three theories are in fairly good agreement as plotted on the logarithmic scales used, but they also indicate considerable scatter when put in terms of seconds, or distance, used during

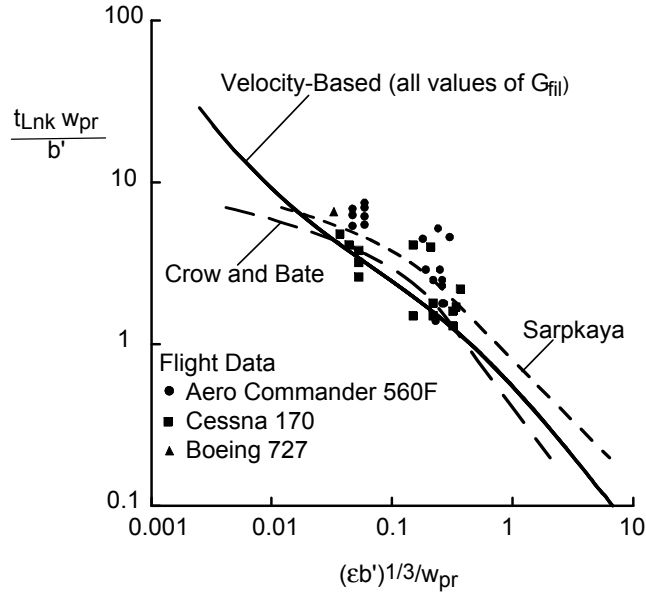


Figure 4. Comparison of predicted linking times as a function of magnitude of disturbance velocities from atmospheric turbulence for long-wave instability of a vortex pair in terms of parameters used by Crow and Bate (ref. 43) and by Sarpkaya (ref. 49).

operations at airports. Some of the scatter in the flight data has been resolved by consideration of the amount of circulation contained in the filament, rather than the entire vortex, but additional parts of the deviations in the data are believed to be associated with the method that was used to measure wind velocity and atmospheric turbulence, and perhaps also due to the fact that the data were taken behind aircraft flying at cruise altitude with robust power (ref. 53). It is believed that a satisfactory method has not yet been determined for measurement of the magnitude of the disturbance velocity parameter to be used in the prediction of wake intrusion into a nearby runway (ref. 20).

If the axes in figure 4 are linear and the dimensionless parameters used for the axes consist of parameters usually used during flight operations at airports, the predictions of vortex linking times appear as indicated in figure 5 (refs. 16 and 20). The velocity-based growth-rate equation includes the possibility that the circulation content of the vortex filaments may not be the same as the estimate based on the maximum content possible just behind the wake-generating wing. The dimensionless circulation parameter, $G_{fil} = \Gamma_{fil} / b_g U_\infty$, in figure 5 covers such a possibility. The velocity-based analysis thereby allows the strength of the vortex pair to differ from the one estimated based on an idealized wake with a single vortex pair. Observations of vortex wakes at cruise altitudes indicate that wakes often divide into several pairs and that the high-speed vortex core is the only part of the vortex wake that participates in the vortex-linking process. Therefore, multiple curves for the strength of the vortex pair going through the linking process are presented in figure 5.

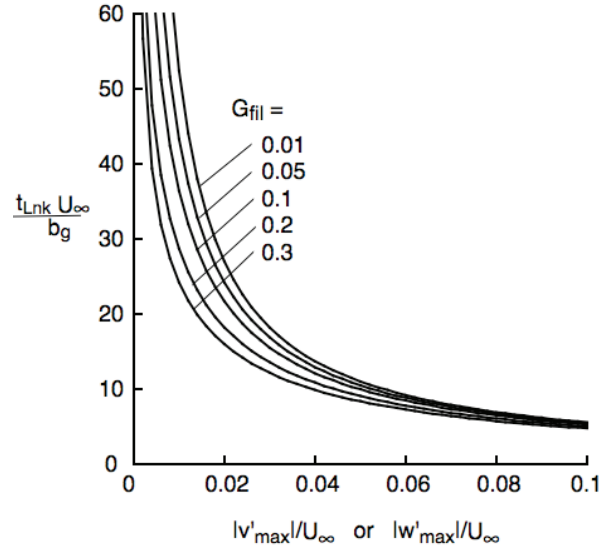


Figure 5. Velocity-based estimate for linking time as a function of magnitude of disturbance velocity for long-wave instability of a vortex pair plotted on linear scales in terms of parameters recommended for applications.

The method used to compute the wake spreading caused by the long-wave instability has been studied in a previous paper (ref. 20), and will therefore only be mentioned here. It is pointed out that wake spreading is a combination of the self-induced and turbulence-induced velocity contributions to the lateral spreading (amplitude of the disturbance wave when viewed in plan view, A_{pln} , and when viewed in face or maximum amplitude as A_{lw}) of the wake due to the long-wave instability. The differential equation is found by use of a combination of equations that describe those quantities as

$$dA_{pln} = [(dA_{lw}/dt)/2]^{1/2} + 2\epsilon_{max}] dt \quad (6a)$$

The dimensionless plan-view amplitude of the waves induced on vortex filaments, A_{pln} , is a function of time, the circulation content of the vortex filaments, Γ_{fil} , and the maximum magnitude of turbulence disturbances, ϵ_{max} , in the atmosphere where the vortices are embedded. Equation (6a) is therefore more complex than the solutions provided by Crow and Bate (ref. 43) and Sarpkaya (ref. 49), and must therefore be integrated numerically to determine a result.

The amplitude of the sinusoidal waves on vortex filaments during the early part of the instability has been observed to not be greatly enhanced by the self-induced velocity field of the long-wave instability until their amplitude exceeds the vortex-linking point (ref. 20). As a result, the amount of wake spreading up to the linking point is approximated by the simple relationship provided by the turbulence-only curves in figure 3. The strong-turbulence form of the linking equations derived by Crow and Bate, and by the velocity-based analysis, can then be used to approximate the spreading of the hazard posed by vortex wakes during the early part of wave formation where turbulence dominates wake spreading, or

$$\tau_{Lnk} \approx (\pi/8)/\varepsilon_{\max} \approx 0.4/\varepsilon_{\max} \quad (6b)$$

where $\tau_{Lnk} = t_{Lnk}U_{\infty}/b_g$ and it is assumed that $\varepsilon_{\max} \approx |v'_{\max}|/U_{\infty} \approx |w'_{\max}|/U_{\infty}$.

D. Self-Induced Downward and Lateral Movement of Vortex Pair

It is assumed that the separation distance between the centroids of the port and starboard vortices is approximated by the value for elliptically loaded wings as $b' \approx \pi b_g/4$. The corresponding value for the self-induced downward velocity of the vortex pair (before wake decomposition begins and when far above the ground plane) is given by

$$w_{pr} = -|\Gamma_{ac}|/2\pi b' \quad (7)$$

where Γ_{ac} is the centerline circulation bound in the wing, which is the same as the magnitude of the total circulation in each of the two vortices in the pair. The magnitude of the downward velocity varies from 1 ft/s (1/3 m/s) for small aircraft to about 10 ft/s (3.05 m/s) for large, heavily loaded aircraft. When the wake-generating aircraft is within about one wing span or less above the ground, the self-induced downward velocity of the vortex pair turns more and more into a lateral velocity so that the spacing between the two vortices becomes larger with time when the vortices are near the ground plane. The maximum value for the lateral velocity occurs when wheel contact is made with the ground. The subsequent self-induced lateral velocity of each vortex adds to the wake-spreading process and must be included in any computation used to determine wake-intrusion time.

When out of ground effect, the shape of the vortex wake can often be approximated by an elliptically shaped region that grows with time as the wake decomposes and spreads. The downward velocity of the wake under those circumstances may then be estimated by a theory based on the downward momentum induced in the wake by the lift force (ref. 17). Therefore, if a value for wake breadth is available from observations (ref. 39) or from theoretical estimates, the downward velocity during wake decomposition and spreading is roughly given by

$$w_{decomp}(t) \approx w_{pr} [B_{oval}/B_{decomp}(t)]^2 \quad (8)$$

where $B_{oval} \approx 2.08 b'/4$ is the initial breadth of the oval-shaped wake, which is usually in a horizontal orientation. The quantity $B_{decomp}(t)$ is the breadth of the decomposing wake (independent of whether its vertical or horizontal extent is largest). Equation (8) indicates that as vortex wakes age their breadth best represents the downward momentum in the wake due to lift on the wake-generating wing. Therefore, as the wake spreads laterally, its descent velocity rapidly becomes smaller.

E. Long-Term Self-Induced Spreading by Turbulence

After the long-wave instability reaches its maximum amplitude, the wake continues to spread as a function of the square root of time due to residual turbulence in the wake itself (ref. 39). In figure 3, the locations where linking and loop formation begin, and where the maximum wave amplitude occurs, are indicated. After maximum amplitude occurs (at about $\tau = 43$), the wake continues to spread as the square root of time as part of its decay process (ref. 39). As a result, the size of the wake-hazardous region continues to increase with time from its initial value because of turbulence, and because of the self-induced velocity field of the long-wave instability of a vortex pair. An empirical relationship for the spreading rate that follows maximum amplitude is now discussed, because long-term avoidance predictions are sometimes needed.

The equation discussed was found from observations made of the condensation trails behind aircraft at cruise altitudes (ref. 39). The equation predicts that, after the long-wave instability has gone to maximum amplitude, the lateral and vertical sizes of the hazardous region are given by

$$B_{hz}(t) \approx D_{hz} \approx b_g C_{hz} (\Delta t)^{1/2} \quad (9)$$

where $C_{hz} \approx 0.5$ is a constant chosen to bring about a best fit to the data and a single curve. The time begins when the wake is generated so that Δt is the time interval in seconds between the generation of the wake and the arrival of a following aircraft at the same along-trail station. Because equation (9) predicts values for the hazardous region that are too small when Δt is small, the breadth and depth of the wake-hazardous region remain constant at their initial values until the sizes predicted by equation (9) are larger values (e.g., fig. 3). At that time, equation (9) is used to predict the location of the outer boundary of the hazardous region. Because equation (9) is not an exact function of the dimensionless parameters used in this paper for the time/distance axis being used, the velocity of the aircraft, U_∞ , is assumed to be 200 ft/s (60.96 m/s) in figure 3, and the span of the aircraft is assumed to be 200 ft, so that the time parameter is equivalent to seconds, or wingspans downstream of the station where the wake was generated.

When all of the contributions to wake spreading are included as shown in figure 3, the $(\Delta t)^{1/2}$ function given by equation (9) applies only after the long-wave instability has reached its maximum amplitude. Because the $(\Delta t)^{1/2}$ function given by equation (9) is then rarely centered on the location of the wake-generating wing, a reference or bias time must be determined so that the predicted breadth of the hazardous region passes through the maximum amplitude point shown on the various figures, at the proper bias time determined so that the curves predicted by equation (9) (with a bias time) pass through the maximum amplitude location. The bias time is determined by modifying equation (9) to read

$$B_{hzmax} = 2y_{maxamp} = C_{hz} (t - t_{bias})^{1/2} b_g \quad (10)$$

where, for $b_f/b_g \leq 0.5$, $B_{hz0} = 2.0$ so that $y_{maxamp}/b_g = 1.0 + \pi/2$ is the maximum amount of wake spreading brought about on each side of the wake centerline by the long-wave instability at the dimensionless time t_{maxamp} . The time is converted to a time in seconds for a specific aircraft

for b_g , and a flight velocity for U_∞ , by use of the relationship, $\tau = t b_g/U_\infty$. Equation (10) passes through the maximum amplitude point when the bias time is given by

$$t_{\text{bias}} = \tau_{\text{bias}} b_g/U_\infty = t_{\text{maxamp}} - (2y_{\text{maxamp}}/b_g C_{\text{hz}})^2 \quad (11)$$

Using equations (10) and (11), the final stage of wake spreading can be extended in figure 3 from the maximum amplitude point downstream to as far as needed.

F. Movement of Wake-Hazardous Boundaries by Wind and Gusts

An aircraft on approach to a set of parallel runways behind a leading aircraft requires a vortex-free flight path along its entire approach path. Therefore, any wind or local gust velocity can cause the locations of vortex segments to move and spread relative to the flight path of the wake-generating aircraft. In this way, the movement and spread of the hazardous region are monitored for an estimate of the size of the safe zone illustrated in figure 1. As discussed previously, it is assumed that the horizontal across-runway components of the wind, and their variations with time or gusts, are obtained along the flight path used by each wake-generating aircraft by use of either ground-based or instrumentation on board the wake-generating aircraft. In figure 6, the upper case letters denote the time-averaged values for the wind components, and the lower case letters denote the maximum unsteady or gust magnitudes in the measurements. Also shown is the self-induced downward velocity of the wake. The motion and spread of wake-hazardous regions predicted by use of maximum measured values of the wind and gust velocities are believed to be conservative, because, as mentioned previously, wind tunnel observations of vortex meander indicate that vortex elements move only about 40% of the amount predicted by wind magnitude (ref. 19). Again, the difference between the two values needs to be studied by use of flight tests.

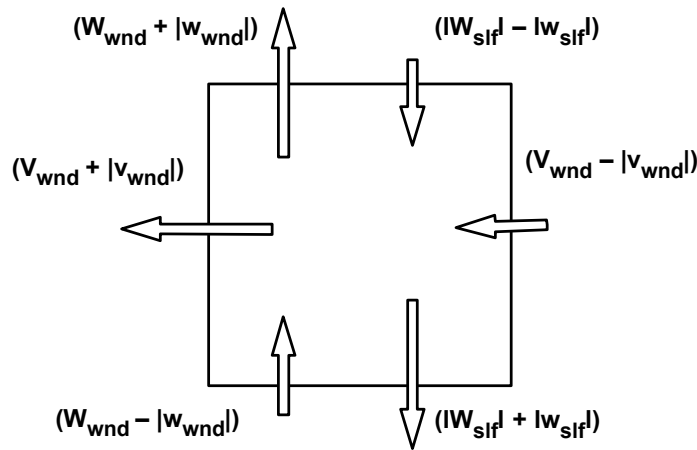


Figure 6. Method used to move cross-sectional boundaries of wake-hazardous region in response to lateral and vertical wind and turbulence disturbance velocity components.

G. Effect of Robust Jet-Engine Exhaust Plumes on Wake Dynamics

As indicated in part A of the Introduction of this paper, it is now known that at least two processes associated with the flight of the aircraft or with ambient turbulence in the atmosphere are able to initiate the long-wave instability of a vortex pair (refs. 42 and 53). The aerodynamic process and an estimate for the duration of the initiation process of this second aerodynamic method are presented in this section. As stated previously, earlier studies on the long-wave instability have attributed the initiation of the long-wave instability of a vortex pair to ambient turbulence in the atmosphere or in the wake of the aircraft. A second initiation process has recently been shown by use of observations and photographs of condensation trails behind aircraft flying at cruise altitudes as the mechanism that usually initiates the long-wave instability when engine thrust is robust. That is, another initiating mechanism is brought about when engine thrust is robust as during take-off, climb, and cruise (refs. 52 and 53). As mentioned in the Introduction, the first step in the second initiating process occurs when an array of circumferential vortices forms around each jet-engine exhaust stream and then merges into a single stream. First, the roll-up of the vortex sheet shed by the lifting wing provides a blanket of exhaust products around the vortex pair that, because of wake roll-up, forms a blanket of exhaust gases around the lift-generated vortex pair. The gaseous blanket then tends to shield the vortex pair from atmospheric turbulence.

Steps towards the initiation of waves along the lift-generated vortex filaments begin when the vortex sheet shed by the wing rolls up into a vortex pair and descends from near the vertical center of the wake to the vicinity of the inside bottom of the combined shear-layer vortex arrays. During this process, the slipstream that forms between the nearly stationary atmosphere and the robust engine exhaust plumes forms into an energetic array of irregularly shaped vortex rings around the combined or merged exhaust plumes from the engines to encase the lift-generated vortex pair. When the vortex pair migrates from just behind the aircraft wing down to the lower inside of the region occupied by the exhaust plumes inside the vortex array, the up and down velocity field of the vortex array causes the axes of the lift-generated vortex pair to become sinusoidal in shape along the flight direction. The sinusoidal shape then serves as ambient turbulence to begin the growth toward the sinuous shapes that lead to the long-wave instability and the across-wake linking that decomposes the flow field of the vortex pair.

As indicated in references 52 and 53, the shielding of the vortices by the engine exhaust plumes and the slow descent of the vortex pair to the bottom of the exhaust vortex array require more time to execute than the atmospheric-turbulence process assumed by Crow (refs. 42, 43 and 44). The atmospheric turbulence process is more rapid because, when robust engine-exhaust plumes are not present, the lift-generated vortex pair is in immediate contact with the turbulence in the ambient atmosphere.

Observations of condensation trails at cruise altitudes indicated that the wave-forming process usually requires 20 s or more and sometimes as much as 2 minutes after aircraft passage. Based on an estimate made in reference 53 for the time for vortex linking to occur when robust engine exhaust plumes are present, the descent time of the vortex pair from just behind that wing near the center of the wake down to the lower inside surface of the array of vortex loops around the

exhaust plumes, and the adjustment time of the wave train to accommodate linking requirements, a *minimum* value for the time to linking the parameter used by Crow is estimated to be about

$$\tau_{\text{Lnk}} = t_{\text{Lnk}} U_{\infty} / b_g \approx 8 \quad (12)$$

where τ_{Lnk} is the dimensionless time parameter introduced by Crow. The numerical value of 8 also indicates the region where linking was observed in several flights of aircraft, which is also just above the theoretical value predicted by Crow and Bate (ref. 43) and Sarpkaya (ref. 49). Such an estimate is in fair agreement with the data taken of condensation trails and labeled flight data (fig. 4). Because wake intrusion times are less when based on ambient turbulence rather than on the value of $\tau_{\text{Lnk}} \approx 8$ or more for cases when engine power is robust, wake intrusion times estimated here will always be based on ambient turbulence because it yields the most conservative value and because engine thrust is usually not used over long periods of time at low levels during approach to a runway.

III. COMPUTATIONAL RESULTS

A. Equations for Wake Spreading

The overall spread and motion of the wake-hazardous region at a given time or distance behind the wake-generating aircraft is based on measured values of ambient turbulence and then determined by use of references 13–20 as

$$\Delta y_{\text{spread}} \approx B_{\text{hz}}(t)/2 + [V_{\text{ave}} + |V_{\text{err}}| + |w_{\text{pr}}|] \Delta t_{\text{ops}} \quad (13)$$

where Δy_{spread} is the amount that the wake-hazardous region has spread in the lateral direction at the time of arrival of a following aircraft. The quantity $B_{\text{hz}}(t)$ is the amount that the wake-hazardous region has spread because of turbulence and the long-wave instability as a function of time. Because $B_{\text{hz}}(t)$ includes the wake-spreading amount caused by turbulence, the contribution brought about by the turbulence in the atmosphere is not entered a second time to the terms inside of the square brackets in equation (13). The parameter Δt_{ops} is the time difference between the arrival of the leading and following aircraft. The parameter V_{ave} represents the lateral velocity of movement of the wake or vortex elements caused by the time-averaged value of the wind component in the across-runway or y-direction. This term calls attention to a choice that can often be made as to whether the following aircraft lands upwind or downwind of the flight path of the preceding aircraft. When the flight path of the following aircraft can be specified as upwind of the flight path of the wake-generating aircraft, the sign of V_{ave} is negative. It is therefore noted that there is considerable advantage in having the following aircraft land upwind of the leading aircraft because the quantity V_{ave} can contribute substantially to the reduction of the wake-spreading rate, and to an increase in the safe allowable along-trail separation distance between aircraft landing in a group. In this way, the time-averaged wind may be called a controllable quantity, because judicious arrangement of aircraft flight paths on approach can make it a beneficial or a detrimental quantity.

The quantity $|V_{err}|$ is an estimate of the accuracy of the various wind and gust magnitudes as measured along the flight path of the wake-generating aircraft. Because measurements at small values are most sensitive to error, it is assumed that it has a value of 5 ft/s ($\approx 2\text{m/s}$). That amount is probably reasonable at low values of wind velocity, and may be conservative for larger wind magnitudes that are of most interest for wake avoidance. An absolute value is used here for the $|V_{err}|$ quantity because it must be assumed to be random and therefore always increases the magnitude of the total amount of wake spreading.

The self-induced downward velocity of the vortex pair that trails from the aircraft wing, w_{pr} , is always positive because, when in ground effect, the port and starboard vortices shed by an aircraft move in an outboard, horizontal direction from the flight path of the wake-generating aircraft. Therefore, the vortex shed by the leading aircraft that is closest to the flight path of the following aircraft always moves to spread the wake. The value of the sum of the lateral velocities in equation (13) is multiplied by Δt_{ops} to yield the total amount estimated for spreading of the wake of the leading aircraft laterally toward the flight path of the following aircraft.

In addition, the magnitude of the maximum gust velocity measured in any direction, $|V_{gust}|_{max}$, is written as a positive quantity so that it will always be used as a positive value in the determination of the maximum measured gust velocities. In this way, the quantity $|V_{gust}|_{max}$ always increases the amount of wake spreading of the wake-hazardous region due atmospheric turbulence and to the long-wave instability as indicated by the last term in equation (6a).

The increase or decrease in wake spreading by an along-runway component of the wind is usually small, because the runway component of the wind simply shifts the wake components toward or away from the touchdown region of the runway surface. Although not included in equation (13), the offset in time experienced by vortex wakes when a wind of a significant magnitude is blowing as a head or tail wind along the approach path of the wake-generating aircraft has been included in the computer program listed in the appendix. Examples calculated for an along-runway component of +10 or -10 ft/s predict that an effect on wake-intrusion time of more than a second is not likely.

The equations for the lateral spread of the hazard posed by vortex wakes clearly indicate the benefits of short time intervals between aircraft operations. First, short time intervals minimize the amount of time available for the wind (and its uncertainties) to move or spread the wake laterally. Second, short intervals of time also reduce the time available for the errors or omissions in wake movement and/or spreading to grow. Minimization of uncertainties makes it possible to operate more efficiently with greater latitude and safety on closely spaced parallel runways, and to increase airport capacity by optimum amounts. Because of the significant number of parameters involved, it is recommended that the maximum allowable time difference before wake intrusion occurs be determined by use of the computer program listed in the appendix, or one like it.

B. Computer Program for Estimation of Wake Spreading

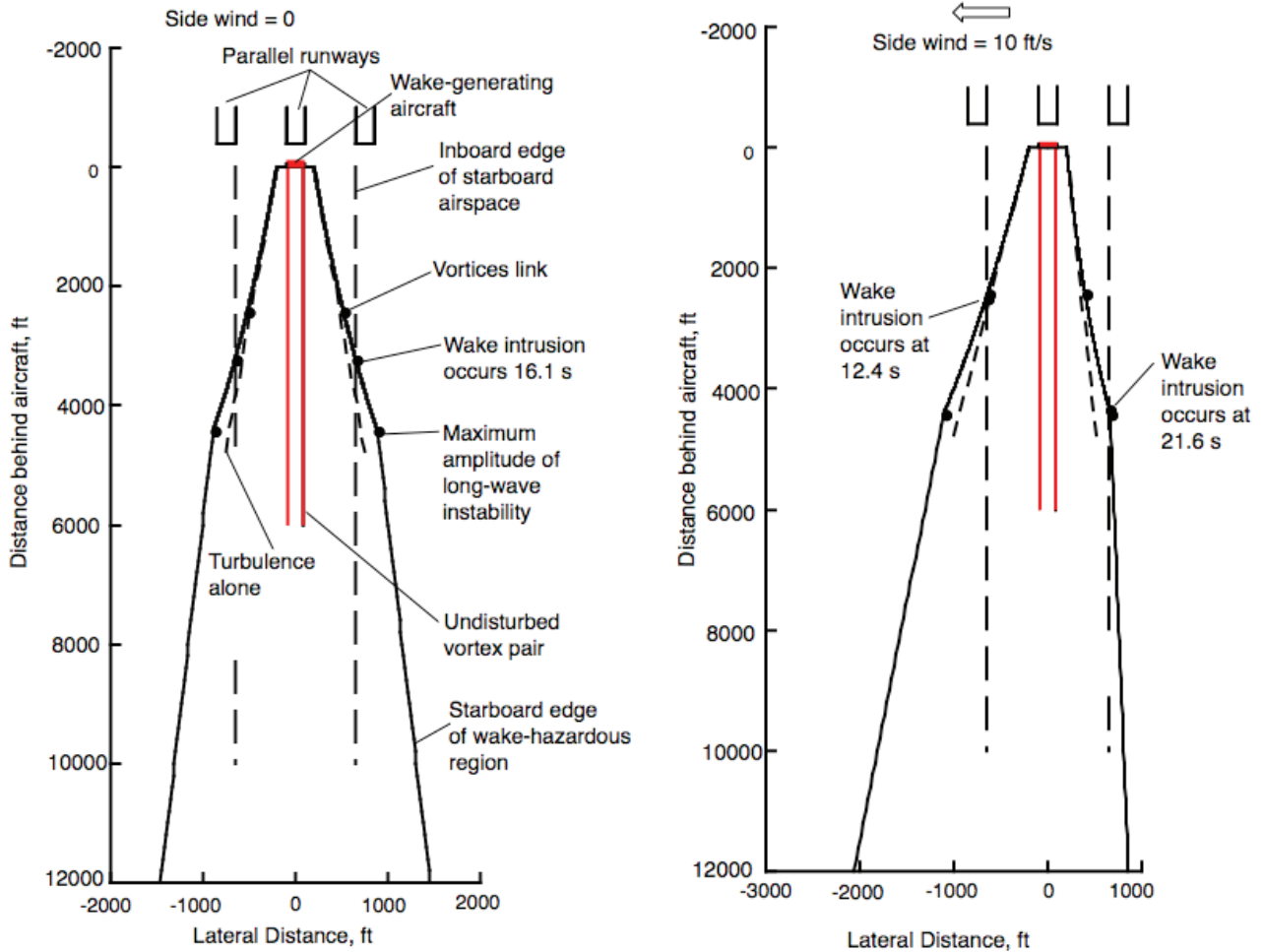
The large number of parameters that enter an estimate for the spreading of the wake-hazardous region as a function of time prompted the development of a computer program or code to expedite the computations needed, to provide a graphical representation of wake spreading in plan view, and to help prevent numerical errors from occurring (see appendix). The computer program begins with the same program used to develop figure 3, which used dimensionless notation throughout. In the computer program, the parameters are first converted from dimensionless notation to feet and seconds where necessary. In the figures presented, the same lines and their associated aerodynamic mechanism shown in figure 3 are presented in figures 7 and 8 to help orient readers as to the dynamics of the wake as it occurs. The resulting computer program is then set up to evaluate the wakes of various aircraft undergoing a variety of atmospheric and airport parameters. The atmospheric parameters used in the several examples shown in figures 7 and 8 include a zero magnitude and a 10 ft/s (3 m/s) side wind for an assumed atmospheric or wake or combined turbulence level of 0.05. The along-runway wind component has been included in the computer program, but it has been set to zero in these figures because it usually has a negligible effect on wake-intrusion times. The two aircraft sizes studied are based on data for early versions of the B-747 and B-737, and may differ from more recent versions now in service.

Both the upwind or windward and downwind or leeward boundaries of the wake-hazardous region are presented on the same figure to indicate the advantages achieved by having following aircraft land on runways *upwind* of the leading aircraft. The two different sizes of aircraft are used to illustrate the advantages achieved by having *smaller* aircraft land ahead of *larger* ones. The closely spaced runways are assumed to be 200 ft (61 m) wide and to have 750 ft (229 m) between their centerlines. Large dots are placed at the locations where vortex linking and maximum amplitude events take place (as in fig. 3), and where wake intrusion into the airspace of nearby runways is predicted to occur—on either the up- or downwind sides of the hazardous region posed by the leading aircraft. Distances behind the wake-generating aircraft are given in feet, and a representative number in terms of seconds is obtained by dividing distance by 200 ft/s (61 m/s), the flight velocity assumed for both the B-747 and the B-737. The computer program and the computations assume that the centerlines of the wake-generating and following aircraft never stray outside of the boundaries defined by the edges of the runway assigned to each of them. In other words, the computations consider only the aerodynamic part of wake avoidance.

Four examples are presented. Readers who may wish to include the techniques described here in their own research may consult the appendix, where a copy of the computer code is listed. The code presented is written in Fortran and was run on a G5 MacIntosh desktop computer with each case taking only a few seconds to run. Such a requirement was indicated when computations were carried out for the simulations made for refs. 31–33 and 54–63.

In the cases presented, a corresponding estimate of the depth of the wake-hazardous region is not made because, although it varies from aircraft to aircraft, it is usually about the same as the magnitude estimated for the lateral spreading amount. Observations of condensation trails behind some aircraft at cruise altitudes indicate that the vertical spreading of vortex wakes may occur more rapidly than the lateral amount. It is assumed in the examples presented, and in the

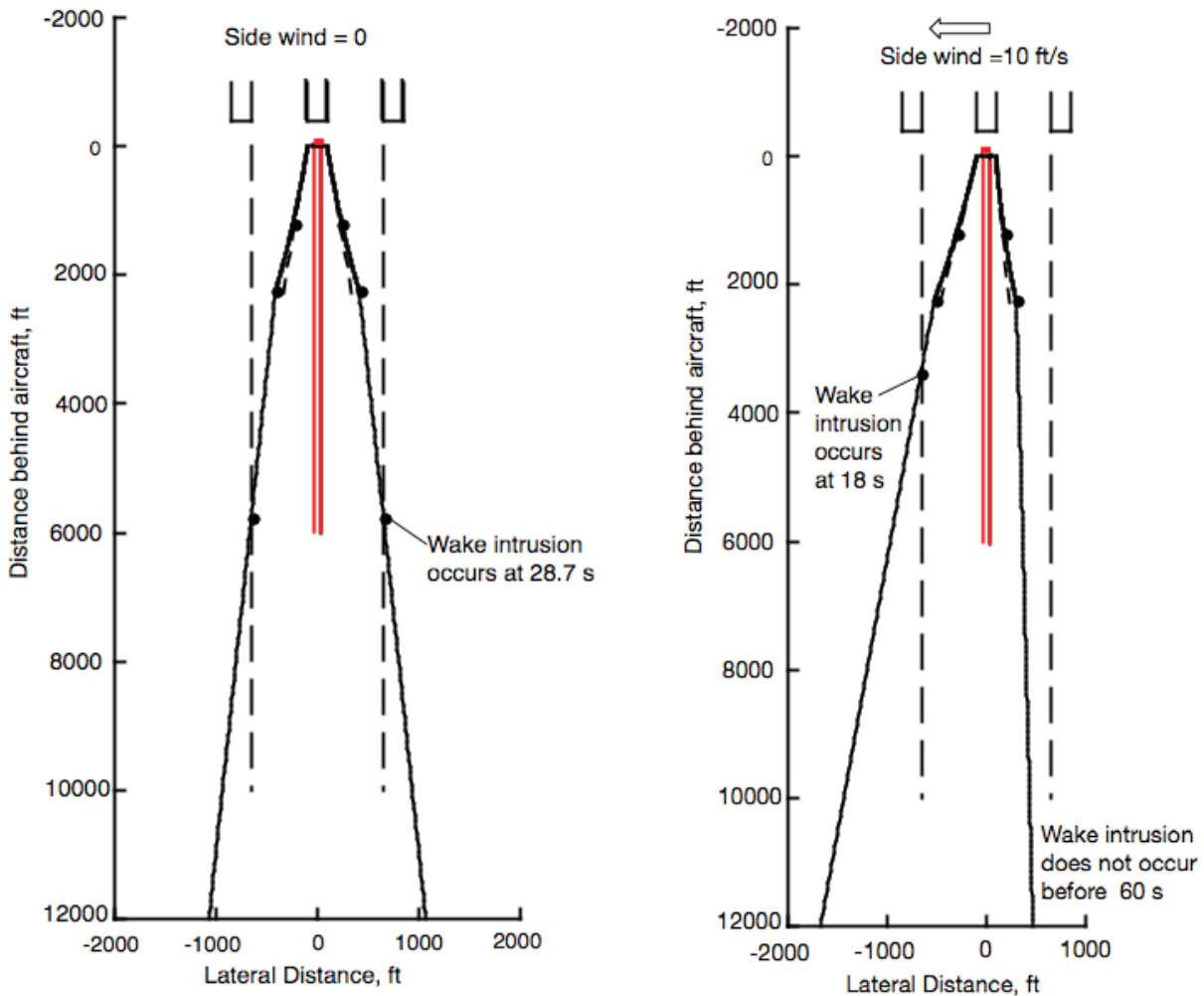
computer code, that the span wise loading on the lifting surfaces of the aircraft is such that the vortex wake rolls up to form a single vortex pair, and that the entire circulation content on one side of the wing goes into the vortex and stays with it throughout the event. Because such an assumption is the most conservative, wake division is not considered (ref. 20).



a) No side wind. Wake intrusion occurs at 3220 ft (16.1 s).

b) Side wind = 10 ft/s (3.05 m). Wake intrusion occurs at about 4320 ft (21.6 s) on windward side and at 2480 ft (12.4 s) on the leeward side of the wake.

Figure 7. Plan view of components of wake-hazardous region shed by B-747 with numbered markers to indicate where various wake-spreading events take place. Computed by using the computer program listed in the appendix with $\epsilon_{\text{eff}} = 0.05$ and $V_{\text{errfs}} = 5 \text{ ft/s}$ (1.52 m). All other wind components are assumed to be of negligible magnitude.



a) No side wind, $\epsilon_{\text{eff}} = 0.05$. Wake intrusion occurs at 5745 ft (28.7 s).

b) Side wind = 10 ft/s, $\epsilon_{\text{eff}} = 0.05$. Wake intrusion occurs at 3375 ft (18 s) on leeward side, and after 12000 ft (60 s) on windward side.

Figure 8. Plan view of components of wake-hazardous region shed by B-737 with numbered markers to indicate where various wake-spreading events take place. Computed by using the computer program listed in the appendix with $\epsilon_{\text{eff}} = 0.05$ and $V_{\text{errfs}} = 5$ ft/s (1.52 m). All other wind components = 0.

IV. IMPLICATIONS FOR AIRPORT OPERATIONS

The aerodynamic guidelines for efficiently avoiding vortex wakes of preceding aircraft are simple. The use of a computer program is recommended so that the large number of parameters that influence wake-intrusion time can be systematically included. If desired, it may then be possible to add any of a number of non-aerodynamic parameters into the computer program to promote safety and an understanding of the disposition of aircraft and runway locations as a

function of time. Because the durations of safe times before wake intrusion are on the order of a few tens of seconds, computer automation of advisory commands and decisions must be used for the determination of aircraft dispositions and guidance.

With regard to how aircraft should efficiently avoid the hazard posed by vortex wakes, both intuition and the information presented in figures 7 and 8 point out that it is advisable to have following aircraft land upwind of preceding aircraft because the side wind then blows wake components away from the flight path of following aircraft. It is also advisable to have smaller aircraft lead larger aircraft, because the cross sections of their wakes are correspondingly smaller, tending to increase the time before wake intrusion occurs, and thus to promote safety. Additional safety is also achieved because larger aircraft can more readily tolerate the wake hazard caused by smaller aircraft. All following aircraft must, of course, comply with the estimates made for wake-intrusion times, and with any non-aerodynamic or operational safety requirements advised for along-trail spacing of aircraft on approach to closely spaced parallel runways at airports. The vertical depth or z-dimension of the wake-hazardous regions is not treated in detail, because it is recommended that all operations be carried out on a sloping planar basis wherein no aircraft ever travels above or below the flight path or active wake of another. It should be remembered that depths of wake-hazardous regions are about the same as their breadths, and wake components often extend above the flight path of the wake-generating aircraft (ref. 8). For these reasons, passage of aircraft above or below preceding aircraft should not be allowed until the wake has positively decomposed. For these reasons, it is also recommended that runway stagger not be used.

The foregoing text dealt with wake-avoidance considerations over only the regions where wake intrusion might be a problem. The analysis and the computer program used to generate figures 7 and 8 dealt with the amount of spreading that occurs in vortex wakes as a function of time. Not analyzed is the time needed for the vortex wakes of an aircraft pair (or group) to decay to a harmless level, so that the airspace previously used is again safe and available for use; i.e., following aircraft must wait for the second safe region shown in figure 1. Called the aerodynamic recycle time for a given set of runways, it represents the time required for the hazard posed by all of the vortex wakes shed by the aircraft pair or group to decay to a harmless level, Δt_{dk} . The form of the computer program used to generate figures 7 and 8, and presented in the appendix, needs a change in objective before it can be used to estimate the recycle time after a set of approaches and landings have been executed. That is, in its present form, the computations estimate the fastest rate at which the hazardous region posed by the wake will spread, and presumably decay. Therefore, the computation may also be used to estimate the shortest time interval required for the vortex wakes to decay to a harmless level. Safety requires, however, that the computation deliver an estimate of the *longest* time interval needed for the decay of the vortex wakes of both aircraft. Because the time interval required for the vortex wakes shed by leading aircraft to decay to a harmless level is uncertain and difficult to estimate, the quantity Δt_{dk} should probably first be set at around three minutes, which is about one and one-half times as long as the longest waiting time now recommended. Flight tests are probably required to determine a more appropriate time interval.

V. CONCLUSIONS

A method is presented, along with a computer program, for estimation of the plan form shape of the outer boundaries of the region within which all of the hazardous elements of lift-generated vortex wakes are located to within a high degree of certainty. The program predicts the amount of along-trail distance or time between arriving aircraft at which the wake of a leading aircraft intrudes into the airspace of a following aircraft for operations on closely spaced parallel runways. The examples presented indicate two simple and obvious rules. First, following aircraft should land upwind of leading aircraft, and secondly, smaller aircraft should precede larger aircraft. The reliability of the predictions for wake-intrusion time depends on how well the components of the time-averaged wind, its gust magnitudes, and the turbulence level along the flight path of each wake-generating aircraft can be measured for an accurate representation of wake spreading as a function of time.

The formulation proposed may be overly conservative, because three assumptions have been made to simplify the method for prediction of the spread of wake-hazardous regions. The first simplification is an assumption that the total circulation in each vortex is the maximum possible, so that the growth rate of the long-wave instability is based on the assumption that the wake contains a single vortex pair of the same strength as initially shed. The second simplification assumes that vortex elements travel with the wind and its larger disturbances without slippage or inertia. This assumption conflicts with observations in wind tunnel tests that show that vortex segments move at about 40% of the disturbance velocities. The third assumption simplifies the measurement of turbulence (or flow-field disturbances) in the atmosphere to a measurement of the maximum (and not the time-averaged) velocity observed in turbulent eddies within the wavelength or frequency range where the long-wave instability is initiated. Because these disturbances may have a time of duration of several tens of seconds, they are referred to as gusts rather than turbulent velocity perturbations. As mentioned previously, the analysis has a non-conservative feature in that it was assumed that any unplanned motions of the wake-generating aircraft be ignored in the computation of the amplitude of wake spreading. Because such motions by an aircraft are unplanned, inclusion in any prediction process is difficult.

Because avoiding vortex wakes is a complicated safety concern and uncertainties exist in the analysis and measurements taken, it is recommended that flight experiments be conducted to better define and confirm the theoretical models being suggested for use in the estimation of the spread of vortex wakes, and the wake-intrusion times that result. The flight experiments should also include measurements of the time required for the decay of the wakes of multiple aircraft in order to better estimate the recycle time for runway systems. The computational method presented is tailored for approach to runways, but the wake-avoidance features analyzed can also be modeled so that they apply to take-off situations if the linking times are modified to those appropriate for robust engine thrust.

VI. REFERENCES

1. Rossow, V.J.: Lift-Generated Vortex Wakes of Subsonic Transport Aircraft. *Progress in Aerospace Sciences*, vol. 35, no. 6, Aug. 1999, pp. 507–660.
2. Spitzer, E.A.; Hallock, J.N.; and Wood, W.D.: Status of the Vortex Advisory System. *Proc. Aircraft Wake Vortices Conf.* J.N. Hallock, ed., Report no. FAA-RD-77-68, U.S. Dept. of Transportation, March 15–17, 1977, pp 326–334.
3. Hinton, D.A.: Aircraft Vortex Spacing System (AVOSS) Conceptual Design. NASA TM-110184, Hampton, Va., Aug. 1995.
4. Rutishauser, D.K.; and O'Connor, C.J.: Aircraft Wake Vortex Spacing System (AVOSS) Performance Update and Validation Study. NASA TM-2001-211240, 2001.
5. Burnham, D.C.; Hallock, J.N.; and Greene, G.C.: Increasing Airport Capacity with Modified IFR Approach Procedures for Close-Spaced Parallel Runways. *Air Traffic Control Quarterly*, vol. 9, no. 1, 2001, pp. 45–58.
6. Hallock, J.N.; and Wang, F.Y.: Summary Results from Long-Term Wake-Turbulence Measurements at San Francisco International Airport. Report no. DOT-VNTSC-FA27-PM-04-13, U.S. Dept. of Transportation, Research and Special Programs Administration, Volpe National Transportation Systems Center, Aviation Safety Division, Cambridge, Mass., July 2004.
7. Hammer, J.: Case Study of Paired Approach Procedure to Closely Spaced Parallel Runways. *Air Traffic Control Quarterly*, vol. 8, no. 3, 1999, pp. 223–252.
8. High Approach Landing System/Dual Threshold Operation, developed by the German Air Safety Provider and Fraport, the Frankfurt Airport company. <http://www.dlr.de/ipa/> and <http://www.pa.op.dlr.de/wirbelschleppe>.
9. Koepp, F.: Doppler Lidar Investigation of Wake Vortex Transport Between Closely Spaced Parallel Runways. *AIAA J.*, vol. 32, no. 4, Apr. 1994, pp. 805–810.
10. Frech, M.; and Holzaepfel, F.: Skill of an Aircraft Wake-Vortex Model Using Weather Prediction and Observation. *AIAA J. of Aircraft*, vol. 45, no. 2, March-April 2008, pp. 461–470.
11. Rahm, S.; Smalikho, I.; and Koepp, F.: Characterization of Aircraft Wake Vortices by Airborne Coherent Doppler Lidar. *AIAA J. Aircraft*, vol. 44, no. 3, May-June 2007, pp. 799–805.
12. Rossow, V.J.: Wake-Vortex Separation Distances When Flight-Path Corridors Are Constrained, *AIAA J. Aircraft*, vol. 33, no. 3, May-June 1996, pp. 539–546.
13. Rossow, V.J.: Reduction of Uncertainties in Prediction of Wake-Vortex Locations. *AIAA J. Aircraft*, vol. 39, no. 4, July-August 2002, pp. 587–596.
14. Rossow, V.J.: Use of Individual Flight Corridors to Avoid Vortex Wakes. *AIAA J. Aircraft*, vol. 40, no. 2, March-April 2003, pp. 225–231.

15. Rossow, V.J.: Implementation of Individual Flight-Corridor Concept. AIAA-2003-6795, AIAA 3rd Aviation, Technology, Integration, and Operations (ATIO) Forum – An Aviation System for the 2nd Century of Flight, Denver, Colo., Nov. 17–19, 2003.
16. Rossow, V.J.; Hardy, G.H.; and Meyn, L.A.: Models of Wake-Vortex Spreading Mechanisms and Their Estimated Uncertainties. AIAA 5th Aviation, Technology, Integration, and Operations (ATIO) Forum, Sept. 26–28, 2005, Arlington, Va., AIAA 2005-7353.
17. Rossow, V.J.: Classical Wing Theory and the Downward Velocity of Vortex Wakes. AIAA J. Aircraft, vol. 43, no. 2, March-April 2006, pp. 381–385.
18. Rossow, V.J.: Vortex-Free Flight Corridors for Aircraft Executing Compressed Landing Operations. AIAA J. Aircraft, vol. 43, no. 5, Sept.-Oct. 2006, pp. 1424–1428.
19. Rossow, V.J., and Meyn, L.A.: Relationship Between Vortex Meander and Ambient Turbulence. AIAA 6th Aviation, Technology, Integration, and Operations (ATIO) Forum, Sept. 25–27, 2006, Wichita, Kans., AIAA 2006-7811.
20. Rossow, V.J.; and Meyn, L.A.: On Data Scatter in Measured Linking Times for Lift-Generated Vortex Pairs. 46th AIAA Aerospace Sciences Meeting and Exhibit, Reno, Nev., Jan. 7–10, 2008, AIAA-2008-0338.
21. Holforty, W.L.; and Powell, D.J.: Flight Deck Display of Airborne Traffic Wake Vortices. 20th Digital Avionics Systems Conference, Daytona Beach, Fla., paper no. 154, Session 2A, Oct. 2001.
22. Hardy, G.H.; and Lewis, E.K.: A Cockpit Display of Traffic Information for Closely Spaced Parallel Approaches. AIAA-2004-5106, AIAA Guidance, Navigation and Control Conference and Exhibit, Providence, R.I., Aug. 16–19, 2004.
23. Moralez, E. III; Tucker, G.E.; Hindson, W.S.; Frost, C.R.; and Hardy, G.H.: In-Flight Assessment of a Pursuit Guidance Display Format for Manually Flown Precision Instrument Approaches.” Am. Helicopter Soc. 60th Annual Forum, Baltimore, Md., June 7–10, 2004.
24. Powell, J.D.; Jennings, C.; and Holforty, W.L.: Use of ADS-B and Perspective Displays to Enhance Airport Capacity. 24th Digital Avionics Systems Conf., Washington, D.C., paper no. 154, session 2A, Nov. 3, 2005.
25. Arkind, K.D.: Maximum Capacity Terminal Area Operations in 2022. AIAA 2003-6791, AIAA 3rd Aviation, Technology, Integration, and Operations (ATIO) Forum – An Aviation System for the 2nd Century of Flight, Denver, Colo., Nov. 17–19, 2003.
26. Miller, M.E.; and Dougherty, S.P.: Communication and the Future of Air Traffic Management. Paper no. 0-7803-8155-6/04, 2004 IEEE Aerospace Conference, Big Sky, Mont., March 6–13, 2004.
27. Arkind, K.: Requirements for a Novel Terminal Area Capacity Enhancement Concept in 2022. AIAA Guidance, Navigation, and Control Conference, Aug. 2004.
28. Miller, M.E.; and Trott, G.A.: Effects of Future Traffic on the National Airspace System. AIAA M&S Conference, Aug. 2004.

29. Miller, M.E.; and Dougherty S.P.: Advanced Terminal Area Communications Link Requirements. 23rd Digital Avionics Systems Conf., Oct. 2004, Salt Lake City, Utah.
30. Miller, M.E.; Dougherty, S.; Stella, J.; and Reddy, P.: CNS Requirements for Precision Flight in Advanced Terminal Airspace. IEEE Aerospace Conf., Mar. 2005.
31. Verma, S.; Lozito, S.; Trot, G.; and Ballinger, D.: Guidelines for Flight Deck Procedures for Very Closely Spaced Parallel Runway Approaches. 27th Digital Avionics Systems Conf., Oct. 26–30, 2008.
32. Cheng, V.H.L.: Airport Surface Operation Collaborative Automation Concept. Proc. AIAA Guidance, Navigation, and Control Conference, Austin, Tex., Aug. 11–14, 2003, AIAA Paper 2003-5773.
33. Cheng, V.H.L.: Research Progress on an Automation Concept for Surface Operation with Time-Based Trajectories. 7th Integrated Communications, Navigation, and Surveillance (ICNS) Conf., Herndon, Va., May 1–3, 2007.
34. Rossow, V.J.; and Tinling, B.E.: Research on Aircraft/Vortex-Wake Interactions to Determine Acceptable Level of Wake Intensity. AIAA J. Aircraft, vol. 25, no. 4, June 1988, pp. 481–492.
35. Rossow, V.J.; Sacco, J.N.; Askins, P.A.; Bisbee, L.S.; and Smith, S.M.: Measurements in 80-by 120-Foot Wind Tunnel of Hazard Posed by Lift-Generated Wakes. AIAA J. Aircraft, vol. 32, no. 2, March-April 1995, pp. 278–284.
36. Rossow, V.J.; Fong, R.K.; Wright, M.S.; and Bisbee, L.S.: Vortex Wakes of Two Transports Measured in 80- by 120-Foot Wind Tunnel. AIAA J. Aircraft, vol. 33, no. 2, March-April 1996, pp. 399–406.
37. Rossow, V.J.: Validation of Vortex-Lattice Method for Loads on Wings in Lift-Generated Wakes. AIAA J. Aircraft, vol. 32, no. 6, Nov.-Dec. 1995, pp. 1254–1262.
38. Schlichting, H.: Boundary-Layer Theory. McGraw-Hill Book Company, 1955, pp. 735–755.
39. Rossow, V.J.; and James, K.D.: Overview of Wake-Vortex Hazards During Cruise. AIAA J. Aircraft, vol. 37, no. 6, 2000, pp. 960–975.
40. Zell, P.T., and Flack, K.: Performance and Test Section Flow Characteristics of the National Full-Scale Aerodynamics Complex 40- by 80-Foot Wind Tunnel. NASA TM-101065, Feb. 1989.
41. Zell, P.T.: Performance and Test Section Flow Characteristics of the National Full-Scale Aerodynamics Complex 80- by 120-Foot Wind Tunnel. NASA TM-103920, Jan. 1993.
42. Crow, S.C.: Stability Theory for a Pair of Trailing Vortices. AIAA J., vol. 8, no. 12, Dec. 1970, pp 2172–2179.
43. Crow, S.C.; and Bate, E.R., Jr.: Lifespan of Trailing Vortices in a Turbulent Atmosphere. AIAA J. Aircraft, vol. 13, no. 7, July 1976, pp. 476–482.
44. Tombach, I.H.: Observations of Atmospheric Effects on Vortex Wake Behavior. AIAA J. Aircraft, vol. 10, no. 11, Nov. 1973, pp. 641–647.
45. Hinze, J.O.: Turbulence, An Introduction to Its Mechanism and Theory. McGraw-Hill Book Co., Inc., 1959, pp. 180–190.

46. Biswas, G.; and Eswaran, V.: *Turbulent Flows, Fundamentals, Experiments and Modeling*. Narosa Publishing House, New Delhi, India, 2002, pp. 44–58.
47. Department of Defense Handbook. *Flying Qualities of Piloted Aircraft*, MIL-STD-1797A, June 28, 1995, Appendix A, 4.9.2 Definition of atmospheric disturbance model form, pp. 678–687.
48. Rossow, V.J.: Prospects for Destructive Self-Induced Interactions in a Vortex Pair. *AIAA J. Aircraft*, vol. 24, no. 7, July 1987, pp. 433–440.
49. Sarpkaya, T.: New Model for Vortex Decay in the Atmosphere. *AIAA J. Aircraft*, vol. 37, no. 1, Jan.-Feb. 2000, pp. 53–61.
50. Hallock, J.N.; and Wang, F.Y.: Summary Results from Long-Term Wake Turbulence Measurements at San Francisco International Airport. Report no. DOT-VNTSC-FA27-1M-04-13, U.S. Dept. of Transportation, Volpe National Transportation Systems Center, Cambridge, Mass., July 2004.
51. Rossow, V.J.; and Meyn, L.A.: Guidelines for Avoiding Vortex Wakes During Use of Closely Spaced Parallel Runways. 26th AIAA Applied Aerodynamics Conf., Honolulu, HI, Aug. 18–21, 2008, AIAA 2008-6907.
52. Rossow, V.J.; and Brown, A.P.: Effect of Jet-Exhaust Streams on Structure of Vortex Wakes. *AIAA J. Aircraft*, vol. 47, no. 3, May-June 2010, pp. 1076–1083.
53. Rossow, V.J.: Initiation of Long-Wave Instability of Vortex Pairs at Cruise Altitudes. NASA TM-2011-216420. Feb. 2011.
54. Verma, S.A.; Lozito, S.; and Trot, G.: Preliminary Guidelines on Flight Deck Procedures for Very Closely Spaced Parallel Approaches. 26th International Congress of the Aeronautical Sciences, ICAS Paper no. 2008-574-Verma-7-01-08, 2008.
55. Verma, S.A.; Lozito, S.; Kozon, T.; Ballinger, D.; and Resnick H.: Evaluation of Triple Closely Spaced Parallel Runway Procedures for Off-Nominal Cases. Eighth USA/Europe Air Traffic Management Research and Development Seminar (ATM2009), June 2009, Napa, Calif.
56. Verma, S.A.; Lozito, S.C.; Ballinger, D.S.; Trot, G.; Hardy, G.H.; Panda, R.C.; Lehmer, R.D.; and Kozon, T.E.: Preliminary Human-in-the-Loop Assessment of Procedures for Very Closely Spaced Parallel Runways. NASA TM-2010-216026, Apr. 2010.
57. Verma, S.A.; Kozon, T.; and Ballinger, D.: Preliminary Guidelines: Air Traffic Control Procedures for Pairing Aircraft for Closely Spaced Simultaneous Approaches. Applied Human Factors Ergonomics Conf., Miami, Fla., paper no. 722, 2010.
58. Verma, S.A.; Lozito, S.; Ballinger, D.; Kozon, T.; Hardy, G.; and Resnick, H.: Comparison of Manual and Autopilot Breakout Maneuvers with Three Closely Spaced Parallel Runway Approaches. Digital Avionics Systems Conf., Orlando, Fla., Oct. 2009.
59. Thippavong, J.; Mulfinger, D.; and Sadovsky, A.: Design Considerations for a New Terminal Area Scheduler. 10th AIAA Aviation Technology, Integration, and Operations (ATIO) Conf., AIAA-2010-9290, Fort Worth, Tex., Sept. 13–15, 2010.

60. Verma, S.A.; Martin, L.; Lozito, S.; Kaneshige, J.; Ballinger, D.; Kozon, T.; Cheng, L.; Sharma, S.; and Subramanian, S.: Integrated Pilot and Controller Procedures: Aircraft Pairing for Simultaneous Approaches to Closely Spaced Parallel Runways. Ninth USA/Europe Air Traffic Management Research and Development Seminar (ATM2011), Berlin, Germany, June 2011.
61. Verma, S.A.; and Farrahi, A.H.: A Pairing Algorithm for Landing Aircraft on Closely Spaced Parallel Runways. Digital Avionics Systems Conf., paper no. 161, Salt Lake City, Utah, Oct. 2010.
62. Verma, S.; Lozito, S.; Kozon, T.; Ballinger, D.; and Resnick, H.: Procedures for Off Nominal Cases: Very Closely Spaced Parallel Runway Operations. Digital Avionics Systems Conf., paper no. 164, St. Paul, Minn., Oct. 2008.
63. Verma, S.A.; Kozon, T.; Ballinger, D.; Lozito, S.; and Subramanian, S.: Role of the Controller in an Integrated Pilot-Controller Study for Parallel Approaches. Digital Avionics Systems Conf., paper no. 343, Seattle, Wash., Oct. 2011.

APPENDIX: COMPUTER CODE FOR WAKE-SPREADING ESTIMATES

It should be noted that the copying process changes the indentation of the various lines of code, and that adjustments may need to be made when the following computer code is copied and pasted onto another computer.

```

      Program W74703
C     AF VERNON J. ROSSOW-
C     MAIN PROGRAM-----W74703.f/WkPlanView
C
C     THIS CODE DEVELOPED TO BE PART OF DISPLAY OF WAKE SPREADING AS A
C     FUNCTION OF TIME TO PROVIDE INFORMATION ON INTRUSION OF
C     WAKE-HAZARDOUS REGIONS INTO AIRSPACE OF A NEARBY PARALLEL RUNWAY.
C
C     Definitions:      alnk = SQRT(2) b'
C                      amax = 5.0*SQRT(2) b'
C                      Alnkbp= alnk/b' = Sqrt(2)
C                      Alnkgb= alnk/bg = Sqrt(2)*PI/4.0
C
C     Program assembles factors that cause wake-hazardous regions of
C     aircraft to move and spread as a function of time. The computer program
C     uses existing theories to estimate the various contributions for the
C     sides of the hazardous region so that it can be plotted in plan view to
C     display the port and starboard boundaries of the hazardous region as a
C     function of time or distance to better visualize how the various
C     contributions affect the along-trail safe zone for safety of operations
C     on closely-spaced parallel runways.
C
C     THIS PROGRAM SETS UP EQUATIONS FOR CALCULATION OF WAKE-SPREADING
C     AS A FUNCTION OF TIME TO ESTIMATE THE TIME AT WHICH THE
C     HAZARDOUS REGION POSED BY VORTEX WAKES WILL INTRUDE INTO THE
C     AIRSPACE OF A NEARBY CLOSELY-SPACED PARALLEL RUNWAY.
C     ALSO COMPUTES TIMES TO VORTEX LINKING, MAXIMUM AMPLITUDE OF LONG-WAVE
C     INSTABILITY AND THE AMPLITUDE OF WAKE SPREADING AS A FUNCTION OF TIME.
C
C     789012345678921234567893123456789412345678951234567896123456789712
C
C     COMMON BG,BGP,N(10),T(101),TT(101),AmplRa(101)
C     1,iout,Tadj(201)
C     2,Tau(4001),Ampbp(4001)
C     3,Ampbg(4001),xplt(20),yplt(20),F2(101)
C     4,Eef(101),TauLn(101),TauMx(101),TauLna(101),TauMxa(101)
C     5,dTauLn(101),dTauMx(101),Amplbp(101),Amplbg(101)
C
C
C     iout = 12
C     IF(iout.ne.6) open(UNIT=iout,FILE='W74703.out')
C
C     PI=ACOS(-1.0)
C     TWOPI=2.0*PI
C     FORPI=4.0*PI
C     PIHAF=PI*0.5
C
C     789012345678921234567893123456789412345678951234567896123456789712
C
C     WRITE(iout,1000)
C     1000 FORMAT(/,'AF VERNON J.ROSSOW  ','W74703.f      April 10, 2008  ')
C           WRITE(iout,1001)
C     1001 FORMAT(/,'STUDY OF AMPLITUDES OF LONG-WAVE INSTABILITY'
C           1,/, 'FOR IMPROVED PREDICTION OF WAKE-INTRUSION TIME'
C           2,/, 'and to calculate the time-history of growth of the long-wave'
```

```

3,/, 'instability of a vortex pair for display purposes.')
```

c

```

c   Parallel projection parameters:
c   THETZ= PI/3.0
c   THELV= PI/6.0
c   DYshft=0.0
```

c

```

c   BG   = WINGSPAN OF WAKE-GENERATING AIRCRAFT
c   BGP  = SPANWISE SEPARATION DISTANCE BETWEEN CENTERS OF VORTEX PAIR.
```

c

```

c   The computations that deal with the dynamics and growth of the
c   long-wave instability need to deal only with the amplitude of the waves
c   in the wave train as as given by a/bg' and the time as given by a
c   combination of circulation and time parameters that reduces to
c   t Gamma/bg'2. These non-dimensional results are then unscrambled so
c   that they can be applied to wake configurations that approximate the
c   dynamics of real wakes behind subsonic transport aircraft when the
c   atmosphere is turbulence and a side wind that is blowing across a
c   nearby runway to be used by a following aircraft.
```

c

```

c   The computations then indicate a time at which the spreading and moving
c   wake of the leading aircraft will intrude into the airspace soon to be
c   used by a following aircraft. This intrusion time dictates the maximum
c   length of time that the following aircraft can following the leading
c   aircraft; that is, the length of the safe zone.
```

c

```

c   Another code was set up to compute the Growth of Wave Amplitude as a
c   function of time for the Long-Wavelength Instability for Range of
c   Ambient Turbulence Levels. From this computation, several constants
c   were generated in order to form a close exponential match to the
c   numerically generated data. The two constants found are given by
c   C1 and C2. These two constants make it possible to calculate the
c   growth rate of the long-wave instability as a function of the
c   current amplitude of the instability. Determination of that derivative
c   makes it possible to calculate the growth of the instability as a
c   function of time. This explains the origin of the two constants used
c   to obtain the amplitude of the long-wave instability; namely
c   C1=0.16579
c   C2=0.04776
```

c

```

c   For turbulence only cases, Gam=0.0.
```

c

```

c   Iter=10
c   Npts=2000
c   Npts=3000
```

c

```

c   AIRCRAFT PARAMETERS for B-747
c   Bgft = 200.0
c   Ufts = 200.0
c   Sft2 = 5500.0
c   Wtlbs= 600000.00
c   Gam  = 4.0*Wtlbs/(0.002378*PI*Ufts*Ufts*Bgft*Bgft)
c   If(Gam.LT.0.0001) Gam=0.0001
c   Wprfts = ABS(2.0*Gam*Ufts/(PI*PI))
```

c

```

c   WRITE(iout,1002) Bgft,Ufts,Sft2,Wtlbs,Gam,Wprfts
1002 Format(/, 'AIRCRAFT PARAMETERS FOR B-747'
1,/, 'Bgft =',F8.2,' Ufts =',F8.2,' Sft2=',F8.2
2,/, 'Wtlbs=',F10.2
3,/, 'Gam=GamND =',F9.5,' Wprfts =',F9.5)
```

c

```

c   ATMOSPHERIC PARAMETERS AT AIRPORT
c   Uwndfs = 0.0
c   Vwndfs = 10.0
```

```

Wwndfs = 0.0
Vgstfs = 0.0
Vgstfs = 0.0
c   Eeff = Vgstfs/Ufts
Eeff = 0.01
VgstES = ABS(Vgstfs-Eeff*Ufts)
VgstES = 0.0
Verrfs = 5.0
c   VgstES is adjusted so that turbulence is not put in twice.
c   Uwndfs is along runway component of atmospheric wind
c   Vwndfs is across runway component of atmospheric wind
c   Wwndfs is vertical component of atmospheric wind--assumed to be zero
c
c   In order to prevent ridiculous gust levels from giving ridiculous
c   wake-intrusion times, a minimum value for Eeff is established at the
c   threshold measurement level. That is, the minimum is set at the
c   lower limit at which a wind velocity can be measured--at our current
c   ability to measure a wind velocity. That value is given by
Eeffmn = Verrfs/Ufts
If(Eeff.LT.Eeffmn) Write(iout, 1033) Eeffmn
If(Eeff.LT.Eeffmn) Eeff = Eeffmn
1033 Format(//, 'ATMOSPHERIC TURBULENCE IS AT MINIMUM THAT CAN BE '
1, 'MEASURED',/, 'Eeff = Eeffmn = ', F10.5)
c
c   VgstES is used in final spreading computations to prevent double
c   emphasis on same turbulence quantities that are present in the
c   atmosphere. The two quantities are being retained as two separate
c   measurements in case the measurement methods find that both Vgstfs and
c   Eeff are important for wake-spreading computations.
c   At this time its is believed that Vgstfs will always be larger than Eeff
c
c   789012345678921234567893123456789412345678951234567896123456789712
c
c   WRITE(iout,1003) Uwndfs,Vwndfs,Wwndfs,Vgstfs,VgstES,Verrfs,Eeff
1003 Format(/, 'ATMOSPHERIC PARAMETERS AT AIRPORT'
1,/, 'Uwndfs =', F8.2, ' Vwndfs =', F8.2, ' Wwndfs =', F8.2
2, ' Vgstfs=', F8.2, ' VgstES=', F8.2
3,/, 'Verrfs =', F10.5, ' Eeff =', F10.5
4,/, 'VgstES is adjusted so that turbulence is not put in twice')
c
c   PARAMETERS FOR AIRPORT SIZE,feet
RnwyBw = 200.0
RnwyCL = 750.0
c   Wake spreading distance to wake intrusion = RnwyCL - 0.5*RnwyBw = WkIntD
WkIntD = RnwyCL - 0.5*RnwyBw
WRITE(iout,1004) RnwyBw,RnwyCL,WkIntD
1004 Format(/, 'PARAMETERS FOR AIRPORT SIZE'
1,/, 'RnwyBw =', F8.2,/, 'RnwyCL =', F8.2,/, 'WkIntD =', F8.2)
c
c   Tau = dimensionless time = t(sec)*Ufts/Bgft
DTau=0.1
c
c   WRITE(iout,4108) Npts,Eeff,Gam,DTau
4108 Format(/, 'Growth of wave amplitude is in diagonal direction until'
1,/, 'downstream distance specified is reached.'
2,/, 'Npts=', I4, ' Eeff=', F9.5, ' Gam=', F9.5
3, ' DTau=', F9.5,/,/, ' J      K      Tau(k)  Ampbg(J,K)  ')
Njump=-1
Do 41 K=1,Npts
Cay=K
Tau(K)=Cay*DTau
If(K.EQ.1) Tau(K)=0.0
If(K.EQ.1) Ampbg(K)=0.0
If(K.EQ.1) Go to 43

```

```

If (K.EQ.2) Ampbg (K) =1.0*Eeff* Tau (K) *Sqrt (2.0)
If (K.EQ.2) Go to 43
Ampbg (K) =Ampbg (K-1) +1.0*Eeff*DTau*Sqrt (2.0)
If (Ampbg (K).LT.0.1) Go to 43
Do 42 I=1, Iter
If (Iter.EQ.1) Ampave = (Ampbg (K) +Ampbg (K-1)) *0.25
If (Iter.GT.1) Ampave = (Ampbg (K) +Ampbg (K-1)) *0.5
DAmp1=0.16579*Gam*Ampave* ((Alog (Ampave/0.04776)) ** (1.0/3.0))
DAmp2=+1.0*Eeff*Sqrt (2.0)
If (DAmp1.LT.0.0) DAmp=DAmp2
If (DAmp1.GT.0.0) DAmp=DAmp1+DAmp2
c Because turbulence increases the spread on both sides of the wake.
c The Sqrt(2.0) is needed because the turbulence spread is added to the
c wave amplification, which is later divided by Sqrt(2.0).
c
c 789012345678921234567893123456789412345678951234567896123456789712
c
Ampbg (K) =Ampbg (K-1) +DAmp* (Tau (K) -Tau (K-1))
42 Continue
43 Continue
c Correction for b'/bg as adjustment to bg references.
Bg = 1.0
Bgp = Bg*PI/4.0
c Linking occurs when a = Sqrt (2) *b'=Sqrt (2) *bg*PI/4.0
c Max amplitude when a = 5*Sqrt (2) *b'=5*Sqrt (2) *bg*PI/4.0
c Write(iout, 4109) J, K, Tau (K), Ampbg (K)
c 4109 Format (2I5, 8F10.5)
If (Njump.GT.0.0) Go to 39
If (Ampbg (K) .GT. (0.5*2.0*Sqrt (2.0)) *PI/4.0) TauLnk= Tau (K)
If (Ampbg (K) .GT. (0.5*2.0*Sqrt (2.0)) *PI/4.0) AmpLnk=Ampbg (K)
If (Ampbg (K) .GT. (0.5*2.0*Sqrt (2.0)) *PI/4.0) NLnk=K
If (Ampbg (K) .GT. (0.5*2.0*Sqrt (2.0)) *PI/4.0) Njump=+1
39 Continue
c
If (Ampbg (K) .GT. (0.5*5.0*Sqrt (2.0)) *PI/4.0) TauMax= Tau (K)
If (Ampbg (K) .GT. (0.5*5.0*Sqrt (2.0)) *PI/4.0) AmpMax=Ampbg (K)
If (Ampbg (K) .GT. (0.5*5.0*Sqrt (2.0)) *PI/4.0) NMax=K
If (Ampbg (K) .GT. (0.5*5.0*Sqrt (2.0)) *PI/4.0) Go to 40
NMax=K
41 Continue
40 Continue
AmpMax=Ampbg (NMax)
TauMax= Tau (NMax)
Write (iout, 4110) NLnk, TauLnk, AmpLnk, Eeff, NMax, TauMax, AmpMax
4110 Format ('Diagonal amplitude of wave is large enough to link:'
1, /, 'NLnk=', I4, ' TauLnk=', F9.4, ' AmpLnk=', F9.4, ' Eeff=', F8.4
2, /, 'NMax=', I4, ' TauMax=', F9.4, ' AmpMax=', F9.4)
c
c PREPARE DATA FOR FIRST PART OF HAZARDOUS BOUNDARY TO LINKING POINT.
Bg=1.0
Bgp=Bg*PI/4.0
BfBg=0.5
c
c 789012345678921234567893123456789412345678951234567896123456789712
c
c Analysis and computations from here on are again based on bg and
c not b'.
c
WRITE (iout, 4111) Eeff, C3, C4, Bg, Bgp, BfBg, Gam, Bgft
4111 FORMAT (/, 'Plan view of growth of Amplitude of Long-Wavelength '
1, 'Instability ', /, 'Numerical Integration for '
2, 'Time History (Dimensionless Notation): '
3, /, 'Eeff=', F9.4, ' C3=', F9.4, ' C4=', F9.4
4, /, 'Bg=', F9.4, ' Bgp=', F9.4, ' BfBg=', F9.4, ' Gam=', F9.4

```

```

5,/, 'Bgft=', F10.2
6,/,/, ' K Tau(K) BHZ BHZHf BHZHm'
7,/,/, ' DATA COMPUTED BUT NOT PRINTED OUT')
c
  If (BfBg.LE.0.5) BHZ0=2.0
  If (BfBg.GT.0.5) BHZ0=2.0+(BfBg-0.5)
  If (BfBg.GE.1.0) BHZ0=2.5
c BHZ0 includes the initial spanwise spacing between vortex centroids
c so that the factor +Bg*PI/4.0 does not need to be added onto BHZ.
  Do 45 K=1,NMax
  BHZ=BHZ0+2.0*Ampbg(K)/Sqrt(2.0)
  BHZHf=0.5*BHZ
  BHZHm=-BHZHf
  If (K.EQ.NLnk) BHZLnk=BHZHf
  If (K.EQ.NMax) BHZMax=BHZHf
c
c WRITE(iout,4112) K, Tau(K), BHZ, BHZHf, BHZHm
c 4112 Format(I4,9F9.4)
  45 Continue
  44 Continue
c
  WRITE(iout,5110) NLnk, TauLnk, AmpLnk, NMax, TauMax, AmpMax
  1, Eeff
5110 Format(/, 'NLnk=', I4, ' TauLnk=', F9.4, ' AmpLnk=', F9.4
  1,/, 'NMax=', I4, ' TauMax=', F9.4, ' AmpMax=', F9.4
  2, ' Eeff=', F9.4)
c
  789012345678921234567893123456789412345678951234567896123456789712
c
c Prepare data for plots of FIRST part of edge of hazardous region
c in terms of feet---that is from aircraft to maximum amplitude of
c long-wave instability.
c
  WRITE(iout,4600)
4600 FORMAT(/, 'Data in seconds and feet---'
  2,/, 'Plan View of Hazardous Region to Max Ampl'
  1,/,/, ' K Tsecs XStn YHZPrt YHZStr')
  IntP = -1
  IntS = -1
  K=0
  Tsecs=0
  XStn =0.0
  YHZPrt=0.0
  YHZStr=0.0
  WRITE(iout,4601) K, Tsecs, XStn, YHZPrt, YHZStr
  Do 46 K=1,NMax
  Tsecs = Tau(K)*Bgft/Ufts
  XStn = Tsecs*(Ufts+Uwndfs)
  BHZ=BHZ0+2.0*Ampbg(K)/Sqrt(2.0)
  YHZPrt=-0.5*BHZ*Bgft - (Vwndfs + VgstES + Verrfs + Wprfts)*Tsecs
  If (IntP.GT.0) Go to 461
  If (ABS(YHZPrt).GT.WkIntD) WkIntP = YHZPrt
  If (ABS(YHZPrt).GT.WkIntD) KIntP = K
  If (ABS(YHZPrt).GT.WkIntD) XStnP = XStn
  If (ABS(YHZPrt).GT.WkIntD) TsecsP = Tsecs
  If (ABS(YHZPrt).GT.WkIntD) IntP = +1
461 Continue
  YHZStr=+0.5*BHZ*Bgft + (-Vwndfs + VgstES + Verrfs + Wprfts)*Tsecs
  If (IntS.GT.0) Go to 462
  If (ABS(YHZStr).GT.WkIntD) WkIntS = YHZSTR
  If (ABS(YHZStr).GT.WkIntD) KIntS = K
  If (ABS(YHZStr).GT.WkIntD) XStnS = XStn
  If (ABS(YHZStr).GT.WkIntD) TsecsS = Tsecs
  If (ABS(YHZStr).GT.WkIntD) IntS = +1

```

```

462 Continue
WRITE(iout,4601) K,Tsecs,XStn,YHZPrt,YHZStr
4601 Format(I5,4F10.2)
If(XStn.GT.12000.0) Go to 54
46 Continue
c
c Compute locations of linking and maximum point for long-wave instab.
c in feet and seconds for plots in real world.
c List data for where linking and maximum values occur in real world.
c
c 789012345678921234567893123456789412345678951234567896123456789712
c
c 789012345678921234567893123456789412345678951234567896123456789712
c
c PREPARE DATA FOR PART OF HAZARDOUS BOUNDARY THAT GOES FROM
c FROM LINKING POINT TO END OF OBSERVATION REGION BY USE OF
c SQRT OF TIME FUNCTION; BHZ = 0.5 BG Sqrt(Adjusted time).
c
c Now extend outer edges of hazardous region further downstream from
c vortex linking point that was just computed. Assume that spreading is
c governed by activity of turbulence generated by aircraft and that
c its effectiveness depends only on its age. Therefore, use Tau values
c for time in the square root term. Do this for a B-747 on approach,
c because then Uinf/bg=1 sec, and Tau or Tac are in seconds or wingspans.
c Information on point of hazardous boundary to be extended is:
c NLnk,TauLnk,AmpLnk,Eeff
c
c BHZ0 includes the initial spanwise spacing between vortex centroids
c so that the factor +Bg*PI/4.0 does not need to be added onto BHZ.
c
c Taupse=Taupseudo=4.0*(BHZ0 + Sqrt(2.0)*AmpMax)**2
c Taupse= 4.0*(BHZ0 + 2.0*AmpMax/Sqrt(2.0))**2
c
c Convert dimensionless data to data in FEET for hazardous boundary
c from Max amplitude of instability to end of computational area.
WRITE(iout,5111)
5111 FORMAT(/,'Growth of wake breadth after maximum amplitude '
1,/,/, ' K Tsecs Xplot YHZEqP YHZEqS')

TauEnd=201.0
TauEnd=100.0
Nmxplt=NMax+200
Do 50 K=NMax,Nmxplt
Cay=K-NMax
Tplot=TauMax+Cay*1.0
Tsecs = Tplot*Bgft/Ufts
Xplot = Tsecs*(Ufts+Uwndfs)
Tac=Taupse+Cay*1.0
BHZ=0.5*Bg*Sqrt(Tac)
YHZPrt=-0.5*BHZ*Bgft - (Vwndfs + VgstES + Verrfs + Wprfts)*Tsecs
If(IntP.GT.0) Go to 4712
If (ABS(YHZPrt).GT.WkIntD) WkIntP = YHZPrt
If (ABS(YHZPrt).GT.WkIntD) KIntP = K
If (ABS(YHZPrt).GT.WkIntD) XStnP = Xplot
If (ABS(YHZPrt).GT.WkIntD) TsecsP = Tsecs
If (ABS(YHZPrt).GT.WkIntD) IntP = +1
4712 Continue
YHZStr=+0.5*BHZ*Bgft + (-Vwndfs + VgstES + Verrfs + Wprfts)*Tsecs
If(IntS.GT.0) Go to 4722
If (ABS(YHZStr).GT.WkIntD) WkIntS = YHZSTR
If (ABS(YHZStr).GT.WkIntD) KIntS = K
If (ABS(YHZStr).GT.WkIntD) XStnS = Xplot
If (ABS(YHZStr).GT.WkIntD) TsecsS = Tsecs
If (ABS(YHZStr).GT.WkIntD) IntS = +1

```

```

4722 Continue
WRITE(iout,5112) K,Tsecs,Xplot,YHZPrt,YHZStr
5112 Format(I4,4F10.2)
If(Xplot.GT.12000.0) Go to 54
50 Continue
54 Continue
C
C 789012345678921234567893123456789412345678951234567896123456789712
C
WRITE(iout,4602)
4602 FORMAT(/,'Data in seconds and feet---'
1,/, 'Plan View of Points where Linking and Maximum Amplitudes'
2, ' occur',/, ' LkMx      Tsecs      XStnft      YHZPLk      YHZSLk')
K = NLnk
TLnk = Tau(K)*Bgft/Ufts
BHZ=BHZ0+2.0*Ampbg(K)/Sqrt(2.0)
YHZPLk=-0.5*BHZ*Bgft - (Vwndfs + VgstES + Verrfs + Wprfts)*TLnk
YHZSLk=+0.5*BHZ*Bgft + (-Vwndfs + VgstES + Verrfs + Wprfts)*TLnk
XStnLk = TLnk*(Ufts+Uwndfs)
WRITE(iout,4603) K,TLnk,XStnLk,YHZPLk,YHZSLk
4603 Format(I5,4F10.2)
C
K = NMax
TMax = Tau(K)*Bgft/Ufts
BHZ=BHZ0+2.0*Ampbg(K)/Sqrt(2.0)
YHZPMx=-0.5*BHZ*Bgft - (Vwndfs + VgstES + Verrfs + Wprfts)*TMax
YHZSMx=+0.5*BHZ*Bgft + (-Vwndfs + VgstES + Verrfs + Wprfts)*TMax
XStnMx = TMax*(Ufts+Uwndfs)
WRITE(iout,4604) K,TMax,XStnMx,YHZPMx,YHZSMx
4604 Format(I5,4F10.2)
C
WRITE(iout,4612)
4612 FORMAT(/,'Data in secs and feet where Hazardous Region Intrudes'
1,/, 'Plan View of Points where Hazardous Region Intrudes'
2, ' occur',/, ' Kint      Tsecs      XInt      WkInt      ')
If(IntP.GT.0) WRITE(iout,4601) KIntP,TsecsP,XStnP,WkIntP
If(IntS.GT.0) WRITE(iout,4601) KIntS,TsecsS,XStnS,WkIntS
C
C
C 789012345678921234567893123456789412345678951234567896123456789712
C
WRITE(iout,7001) BHZ0
7001 FORMAT(/,'BHZ0=',F10.2)
1,/, 'Spread of Haz. region in FEET due to turbulence only '
2,/,/, ' J      Tsecs      Xplot      YTurBP      YTurBS')
C
do 71 J=1,21
Yay=J-1
Tsecs = 2.0*Yay
Xplot= Tsecs*(Ufts+Uwndfs)
BHZ=BHZ0*Bgft+2.0*Eeff*Xplot
YTurBP=-0.5*BHZ - (Vwndfs + VgstES + Verrfs + Wprfts)*Tsecs
YTurBS=+0.5*BHZ + (-Vwndfs + VgstES + Verrfs + Wprfts)*Tsecs
WRITE(iout,5112) J,Tsecs,Xplot,YTurBP,YTurBS
7002 Format(I4,9F10.2)
If(Xplot.GT.XStnMx) Go to 72
71 Continue
72 Continue
C
C End of data listing for plot of boundaries of hazardous region.
C
C 789012345678921234567893123456789412345678951234567896123456789712
C
C Set up reference lines for wing and wake--in terms of FEET.

```

```

Chord = 0.25*Bgft
xplt(1) = 6000.0
yplt(1) = -0.5*Bgft*(PI/4.0)
xplt(2) = 0.0
yplt(2) = -0.5*Bgft*(PI/4.0)
xplt(3) = 0.0
yplt(3) = +0.5*Bgft*(PI/4.0)
xplt(4) = 6000.0
yplt(4) = +0.5*Bgft*(PI/4.0)
xplt(5) = 0.0
yplt(5) = +0.5*Bgft*(PI/4.0)
c
xplt(6) = 0.0
yplt(6) = +0.5*Bgft
xplt(7) = 0.0-Chord
yplt(7) = +0.5*Bgft
xplt(8) = 0.0-Chord
yplt(8) = -0.5*Bgft
xplt(9) = 0.0
yplt(9) = -0.5*Bgft
c
c
WRITE(iout,6001)
6001 FORMAT(/,'Reference lines for Wake and Wing Layout '
1,/,/, ' J xwnwk ywnwk ')
do 61 J=1,9
WRITE(iout,6002) J,xplt(J),yplt(J)
6002 Format(I4,9F10.2)
61 Continue
c
c
c Set up reference lines for three runways--in terms of FEET.
c First runway:
xplt(1) = -5.0*RnwyBw
yplt(1) = -0.5*RnwyBw
xplt(2) = -2.0*RnwyBw
yplt(2) = -0.5*RnwyBw
xplt(3) = -2.0*RnwyBw
yplt(3) = +0.5*RnwyBw
xplt(4) = -5.0*RnwyBw
yplt(4) = +0.5*RnwyBw
c
WRITE(iout,8001)
8001 FORMAT(/,'Reference lines for Runway for Wake-Gen Aircraft'
1,/,/, ' J xrnw1 yrnw1 ')
do 81 J=1,4
WRITE(iout,8002) J,xplt(J),yplt(J)
8002 Format(I4,9F10.2)
81 Continue
c
c Port runway:
xplt(1) = -5.0*RnwyBw
yplt(1) = -0.5*RnwyBw - RnwyCL
xplt(2) = -2.0*RnwyBw
yplt(2) = -0.5*RnwyBw - RnwyCL
xplt(3) = -2.0*RnwyBw
yplt(3) = +0.5*RnwyBw - RnwyCL
xplt(4) = -5.0*RnwyBw
yplt(4) = +0.5*RnwyBw - RnwyCL
c
WRITE(iout,8003)
8003 FORMAT(/,'Reference lines for Runway on Port Side'
1,/,/, ' J xrnw2 yrnw2 ')
do 82 J=1,4

```

```

      WRITE(iout,8004) J,xplt(J),yplt(J)
8004 Format (I4,9F10.2)
82   Continue
c
c
c   Starboard runway:
      xplt(1) =-5.0*RnwyBw
      yplt(1) =-0.5*RnwyBw + RnwyCL
      xplt(2) =-2.0*RnwyBw
      yplt(2) =-0.5*RnwyBw + RnwyCL
      xplt(3) =-2.0*RnwyBw
      yplt(3) =+0.5*RnwyBw + RnwyCL
      xplt(4) =-5.0*RnwyBw
      yplt(4) =+0.5*RnwyBw + RnwyCL
c
      WRITE(iout,8013)
8013 FORMAT(/,'Reference lines for Runway for Following Aircraft-feet'
1,/,/, ' J      xrnw3      yrnw3  ')
      do 812 J=1,4
      WRITE(iout,8014) J,xplt(J),yplt(J)
8014 Format (I4,9F10.2)
812   Continue
c   789012345678921234567893123456789412345678951234567896123456789712
c
c   Wake Intrusion Lines at Inner Side of Airspace for Following Aircraft:
c   Port side.
      Xplt(1) = 0.0
      Yplt(1) =-(RnwyCL-0.5*RnwyBw)
      Xplt(2) = 50.0*Bgft
      Yplt(2) =-(RnwyCL-0.5*RnwyBw)
c
      WRITE(iout,8005)
8005 FORMAT(/,'Port Wake Intrusion Line for Following Aircraft-feet'
1,/,/, ' J      XintP      YintP  ')
      do 83 J=1,2
      WRITE(iout,8006) J,Xplt(J),Yplt(J)
8006 Format (I4,9F10.2)
83   Continue
c
c   Starboard side.
      Xplt(1) = 0.0
      Yplt(1) =+(RnwyCL-0.5*RnwyBw)
      Xplt(2) = 50.0*Bgft
      Yplt(2) =+(RnwyCL-0.5*RnwyBw)
c
      WRITE(iout,8007)
8007 FORMAT(/,'Strbd Wake Intrusion Line for Following Aircraft-feet'
1,/,/, ' J      Xints      Yints  ')
      do 84 J=1,2
      WRITE(iout,8006) J,Xplt(J),Yplt(J)
84   Continue
c   789012345678921234567893123456789412345678951234567896123456789712
c
c
c   703 STOP
      END
c

```